Regulation and role of endoglin in cholesterol-induced endothelial/vascular dysfunction *in vivo* and *in vitro*

Matej Vicen[1ϕ], Barbora Vitverova[1ϕ], Radim Havelek[2], Katerina Blazickova[1], Miloslav Machacek[3], Jana Rathouska[1], Iveta Najmanová[1], Eva Dolezelova[1], Alena Prasnicka[1], Magdalena Sternak[4], Carmelo Bernabeu[5], Petr Nachtigal[1]

[1] Charles University, Faculty of Pharmacy in Hradec Kralove, Department of Biological and Medical Sciences, Hradec Kralove, Czech Republic

[2] Charles University, Faculty of Medicine in Hradec Kralove, Department of Medical Biochemistry, Hradec Kralove, Czech Republic

[3] Charles University, Faculty of Pharmacy in Hradec Kralove, Department of Biochemical Sciences, Hradec Kralove, Czech Republic

[4] Jagiellonian Centre for Experimental Therapeutics (JCET), Bobrzynskiego 14, 30-348, Krakow, Poland

[5] Center for Biological Research, Spanish National Research Council (CSIC) and Biomedical Research Networking Center on Rare Diseases (CIBERER), Madrid, Spain

Short title: endoglin, cholesterol and endothelial dysfunction

***Corresponding author:** Nachtigal Petr, PhD; Department of Biological and Medical Sciences, Faculty of Pharmacy in Hradec Kralove, Charles University, Heyrovskeho 1203, Hradec Kralove 500 05, Czech Republic

E-mail address: petr.nachtigal@faf.cuni.cz

Phone/fax numbers: +420495067305/ +420495067170

[ϕ] These authors contributed equally to this work

1. ABBREVIATIONS

7K	7-ketocholesterol
$ApoE^{-/-}/LDLR^{-/-}$	ApoE/LDLR-deficient mouse strain
Eng	Endoglin
eNOS	Endothelial nitric oxide synthase
GAPDH	Glyceraldehyde 3-phosphate dehydrogenase
GW4869	N,N′-Bis[4-(4,5-dihydro-1H-imidazol-2-yl)phenyl]-3,3′-*p*-phenylene-bis-acrylamide dihydrochloride
HAECs	Human aortic endothelial cells
HIF-1α	Hypoxia inducible factor 1α
HO-1	Heme oxygenase-1
ICAM-1	Intercellular cell adhesion molecule 1
KLF6	Krűppel-like factor 6
L-NAME	N (ω)-nitro-L-arginine methyl ester
LXR	Liver X nuclear receptor alpha variant 1 member 3
MMP-14	Matrix metalloproteinase-14
NF-κB	Nuclear factor kappa B
NR1H3	Liver X nuclear receptor alpha variant 1 member 3 gene
NO	Nitric oxide
NO_2^-	Nitrite
NO_3^-	Nitrate
PE	Phenylephrine
p-eNOS	Phosphorylated endothelial nitric oxide synthase
PHA-408	8-[[5-chloro-2-(4-methylpiperazin-1-yl) pyridine-4-carbonyl] amino]-1-(4-fluorophenyl)-4, 5-dihydrobenzo[g]indazole-3-carboxamide
pMLC Thr18/Ser19	Phosphorylated myosin light chain Threonine18/Serine19
pSmad2/3	Phosphorylated Smad2/3
RELA	NF-κB phosphorylated on carbon 65
sEng	Soluble endoglin
SNP	Sodium nitroprusside
THP-1	Human acute monocytic leukemia cell line
TNF-α	Tumor necrosis factor alpha
WT	Wild type C57BL/6J mouse strain

ABSTRACT

Objective: To investigate the effect of cholesterol (hypercholesterolemia/7-ketocholesterol) on endoglin expression and regulation with respect to endothelial/vascular dysfunction *in vivo* and *in vitro*.

Approach and results: *In vivo* experiments were performed in two-month-old ApoE$^{-/-}$/LDLR$^{-/-}$ female mice and their wild type C57BL/6J littermates. In *in vitro* experiments, Human Aortic Endothelial Cells (HAECs) were treated with 7-ketocholesterol (7K).

ApoE$^{-/-}$/LDLR$^{-/-}$ mice developed hypercholesterolemia accompanied by increased circulating levels of P-selectin and endoglin and a disruption of NO metabolism. Functional analysis of aorta demonstrated impaired vascular reactivity and Western blot analysis revealed downregulation of membrane Eng/Smad2/3/eNOS signaling in ApoE$^{-/-}$/LDLR$^{-/-}$ mice. 7K increased endoglin expression via KLF6, LXR and NF-κB in HAECs. 7K-induced endoglin expression was prevented by the treatment with 2-hydroxypropyl-β-cyclodextrin, PHA-408 or by KLF6 silencing. 7K induced increased adhesion and transmigration of monocytic THP-1 cells, was prevented by endoglin silencing.

Conclusions: Hypercholesterolemia altered endoglin expression and signaling, followed by endothelial/vascular dysfunction before formation of atherosclerotic lesions in ApoE$^{-/-}$/LDLR$^{-/-}$ mice. By contrast, 7-ketocholesterol increased endoglin expression, and induced inflammation in HAECs, which was followed by an increased adhesion and transmigration of monocytes via endothelium, which was prevented by endoglin inhibition. Thus, we propose a relevant role for endoglin in endothelial/vascular dysfunction/inflammation when exposed to cholesterol.

Key words: Endoglin; Hypercholesterolemia; Oxysterols; Endothelial dysfunction; Mice

2. INTRODUCTION

Endoglin (Eng), also known as CD105 and TGF-β receptor III, is a homodimeric transmembrane glycoprotein, that is predominantly expressed in arterial endothelial cells (1). It is an important regulator of TGF-β signaling in different physiological/pathological conditions. Moreover, a soluble form of endoglin (sEng) is released into the blood circulation after proteolytic cleavage of juxtamembrane region of membrane-bound Eng (2) in various pathological conditions with potential involvement of matrix metalloproteinase-14 (MMP-14) as the major endoglin shedding protease (3).

Membrane Eng expression is regulated by various transcription factors including KLF6 (member of the zinc finger Krűppel-like factor family ubiquitously expressed in human tissues) (4), RELA (p65 NF-κB) - Hypoxia inducible factor 1α (HIF-1α) (inflammatory and oxidative stress pathway factors) (5-7) and Liver X receptor (LXR; cholesterol metabolism related factor and oxysterol receptor) (8). In addition, it has been shown that Eng is involved in Smad2/3 phosphorylation (signaling), which results in regulation of expression and proper function of endothelial nitric oxide synthase (eNOS) in endothelial cells and demonstrates a relationship between Eng and nitric oxide (NO)-dependent vasodilation (9, 10). Thus, Eng might be considered as a vasoprotective or endothelium protective agent. On the other hand, membrane Eng and sEng were proposed to be ligands for leukocyte integrins. It was suggested that Eng might participate in integrin-mediated inflammatory infiltration of leukocytes (11) and platelet adhesion to endothelium (12).

Hypercholesterolemia and/or increased levels of oxidized LDL (oxLDL) are crucial inducers of development of endothelial dysfunction, which is followed by atherogenesis as shown in experimental animal models, as well as in humans (13). Cholesterol in blood especially the one accumulated in arterial intima can be modified by different mechanisms resulting in formation of oxysterols. Low density lipoprotein particles (LDL) contain predominantly oxysterols of non-enzymatic origins. Among these, 7-ketocholesterol (7K) is a typical representative (14) and it is one of the most common oxysterols present in healthy human plasma (15). In addition, it was demonstrated that 7K promotes inflammation (16) and foam cell formation (17).

We previously demonstrated that Eng expression is detected only in endothelial cells in aorta in mouse model of atherosclerosis (1). Moreover, membrane Eng expression was reduced

in advanced atherosclerotic plaques, while sEng levels were increased (18, 19). In addition, membrane Eng expression was decreased and sEng levels were increased, when human umbilical vein endothelial cells were exposed to inflammatory stimulation by TNF-α for 24 hours (20). Interestingly, membrane Eng and sEng were shown to participate in inflammatory infiltration of leukocytes both *in vivo* and *in vitro* (11, 21). These data suggest a complex regulated expression and function of Eng during endothelial dysfunction/inflammation, which are key early steps of atherogenesis.

Above mentioned data clearly show discrepancies in the potential endoglin role in *in vivo* studies simulating atherogenenesis (macrocirculation) and *in vitro* studies focusing on different blood vessels (microcirculation).

Thus, in this paper we aimed to combine *in vivo* and *in vitro* approach and focus on regulation of endoglin expression and endoglin related signaling in aortic endothelial cells (mouse aorta and human aortic endothelial cells) under the "cholesterol attack" in order to elucidate endoglin role in endothelial function/dysfunction.

Therefore, in the first part of this study, we hypothesized that hypercholesterolemia alters endoglin expression/signaling with respect to endothelial function in aorta before formation of any atherosclerotic changes in wild type C57BL/6J (WT) and hypercholesterolemic ApoE/LDLR-deficient ($ApoE^{-/-}/LDLR^{-/-}$) mice. In the second part, using human aortic endothelial cells we hypothesized that 7-ketocholesterol (mimicking hypercholesterolemia) affects membrane Eng expression and its involvement in monocyte adhesion/transmigration *in vitro*.

The results of this manuscript showed for the first time three main outcomes: 1) Hypercholesterolemia altered endoglin expression and signaling followed by endothelial/vascular dysfunction before the formation of atherosclerotic changes in aorta (previous papers showed alteration of endoglin expression and signaling but without functional consequences and in aorta with advanced atherosclerotic lesions); 2) 7-ketocholesterol (simulating ox-LDL effects in *in vivo* experiments)-induced increase in endoglin expression was regulated by simultaneous activation of three transcription factors including KLF6, RELA (NF-κB) and NR1H3 (LXR); and 3) Endoglin might be involved in cholesterol induced adhesion/transmigration of monocytes via endothelium.

3. MATERIALS AND METHODS

3.1. Animals and experimental design

ApoE$^{-/-}$/LDLR$^{-/-}$ female mice (n=7 in each group), the model initially described by (22) and extensively characterized in previous studies (23, 24) , were used in the current study at the age of two months. C57BL/6J (WT) female mice (n=7 in each group) were used for comparison and were obtained from the Jackson Laboratory (Bar Harbor, ME, USA). It is of interest to mention that in our hands female mice are easier to breed than male mice all our previous studies with ApoE-/-/LDLR-/- mice were performed with female mice for consistency and comparative purposes. The animals were kept in controlled ambient conditions in a temperature-controlled room with a 12h-12h light-dark cycle with constant humidity and had access to tap water and standard chow diet *ad libitum*. WT and ApoE$^{-/-}$/LDLR$^{-/-}$ mice were not cohoused in the same cages. At the age of 8 weeks, mice were euthanized under general anesthesia induced by a combination of xylazine (10 mg/kg intraperitoneally) and ketamine (100 mg/kg intraperitoneally), and blood, urine and aorta samples were harvested for further analysis.

All experiments were carried out in accordance with the standards established in the directive of the EU (2010/63/EU) and all procedures were approved by the Ethical Committee for the protection of animals against cruelty at Faculty of Pharmacy, Charles University (Permit Number: 21558/2013-2).

3.2. Cell culture

Human aortic endothelial cells (HAECs) are primary cells from pooled donors purchased from Lonza (Basel, Switzerland). HAECs were cultured on Petri dishes (TPP, Trasadingen, Switzerland) coated with gelatin (Sigma-Aldrich, Darmstadt, Getmany) in endothelial growth media (EGM™-2, Lonza, Basel, Switzerland) with adequate supplements (Lonza, Basel, Switzerland) and 10% fetal bovine serum (FBS; Sigma, Darmstadt, Germany) at 37°C and 5% CO_2. Gelatin acts as extracellular matrix and helps HAECs to attach to the bottom of Petri dishes. All experiments were performed with HAECs passage 5 (cumulative population doubling 9-10). To avoid cell-cell contact inhibition, HAECs were passaged or premedicated after reaching of 80-90% confluence.

The human leukemia pro-monocytic cell line (THP-1), with features of monocytes derived from blood plasma, was kindly provided by Soňa Čejková (Institute for Clinical and

Experimental Medicine, Prague, Czech Republic) and used to study the effects of 7-ketocholesterol (7K). THP-1 cells were cultured in RPMI 1640 medium (Thermo Fisher Scientific, Waltham, MA, USA) supplemented with penicillin/streptomycin (Sigma-Aldrich, Darmstadt, Germany), glutamine (Glutamax, Thermo Fisher Scientific, Waltham, MA, USA) and 10% FBS (Sigma-Aldrich, Darmstadt, Germany) in non-adhesive flasks (SPL Life Sciences, Gyeonggi-do, Korea). Cell density was maintained at a concentration of 0.1-0.9 million cells per milliliter of medium. For amplification, cells were split 1:3 after reaching a density of 0.8-0.9 million cells per milliliter.

3.3. Chemicals

7-ketocholesterol (7K), 2-hydroxypropyl β-cyclodextrin, PHA-408 (8-[[5-chloro-2-(4-methylpiperazin-1-yl) pyridine-4-carbonyl] amino]-1-(4-fluorophenyl)-4, 5-dihydrobenzo[g]indazole-3-carboxamide) and GW4869 **(**N,N′-Bis[4-(4,5-dihydro-1H-imidazol-2-yl)phenyl]-3,3′-*p*-phenylene-bis-acrylamide dihydrochloride) were purchased from Sigma-Aldrich (Darmstadt, Germany). Solutions of 7K were prepared just before cell premedication at 10μg/mL using 100μL ethanol (Penta, Praha, Czech Republic) as cosolvent to dissolve 1mg of oxysterol in culture medium. The same amount of ethanol was added to control samples. Stock solution of PHA-408 was prepared using DMSO (Sigma-Aldrich, Darmstadt, Germany) 25μL/125μg. Treatments were done with medium containing 10% FBS. To analyze acute effects of oxysterols, we used doses of 5 and 10μg/mL. Dosage was selected according to preliminary dose and time dependent experiments (data not shown) and previously published paper (25). 2-hydroxypropyl β-cyclodextrin (for the inhibition of NR1H3/LXR) and PHA-408 (for the inhibition of NF-κB) were used at a final concentration of 10mM and 10μM, respectively.

3.4. Biochemical analysis

Total concentration of plasma cholesterol was measured enzymatically by conventional enzymatic diagnostic kits (Lachema, Brno, Czech Republic) and spectrophotometric analysis (cholesterol at 510 nm, ULTROSPECT III, Pharmacia LKB Biotechnology, Uppsala, Sweden).

3.5. Luminex assay

Blood samples from mice were obtained from vena cava inferior and plasma levels of mouse sEng and soluble P-selectin were determined by means of a Mouse Premixed Multi-Analyte Magnetic Luminex Kit (R&D Systems, MN, USA), according to the manufacturer's protocol.

3.6. Measurement of plasma and urinary concentration of nitrate

The concentration of nitrate (NO_3^-) in plasma and urine was measured by an ENO-20 NOx Analyzer (Eicom Corp., Kyoto, Japan). The analysis is based on a liquid chromatography method with post-column derivatization using Griess reagent. NO_3^- was separated from other substances in matrices on a NO-PAK column (4.6 x 50mm Eicom Corp., Kyoto, Japan). Then, NO_3^- was reduced to nitrite (NO_2^-) using a cadmium-copper column (NO-RED, Eicom Corp., Kyoto, Japan). Subsequently, NO_2^- was mixed with Griess reagent to form a purple azo dye in reaction coil placed in a column oven at 35°C. The absorbance of derivatives was measured at 540 nm. The flow rate of the mobile phase (Carrier Solution) was 330 μL/min. The Griess reagent (Reactor A and B Solution 1:1, v/v) was delivered by a pump at a flow rate of 110 μL/min. Plasma samples were precipitated with methanol at a ratio of 1:1 (v/v), centrifuged at 10000xg for 10 min, and the resulting supernatant was analyzed. To measure urinary nitrate concentration, urine samples were diluted 5-fold and analyzed directly (26, 27).

3.7. Functional analysis of vascular reactivity *ex vivo*

Aortic rings underwent cleaning, mounting and measuring processes as described previously (28). The change of contractile substance is the only difference from previous protocol. Aortic rings were pre-contracted with increasing concentrations of phenylephrine (PE, 0.01-10 μM).

3.8. Western blot analysis

The procedure was performed as reported previously (29).

3.9. Elisa

HAECs were treated with 5 µg/mL or 10 µg/mL of 7K for 12 hours and culture supernatants were collected and analyzed by ELISA assay (Bio-Techne R&D Systems, DNG00 Human endoglin/CD105 Quantitative ELISA Kit, Minneapolis, MN, USA). Concentration of sEng was determined according to manufacturer's protocol.

3.10. Quantitative real-time PCR

HAECs were treated with 5 µg/mL or 10 µg/mL of 7K for 12 hours. The mRNA expression of glyceraldehyde 3-phosphate dehydrogenase (*GAPDH* Hs02758991_g1), *membrane endoglin* (Hs00923996_m1), *NR1H3* (Hs00172885_m1), *KLF6* (Hs00810569_m1), *RELA* (Hs00153294_m1), *eNOS* (Hs00167166_m1) and *ICAM-1* (Hs00164932_m1) (all provided by Life Technologies, Foster City, CA, USA) was evaluated using qRT-PCR. KLF6 and endoglin silencing and treatment with either 2-hydroxypropyl-β-cyclodextrin or PHA-408 were followed by evaluation by means of the same set of genes. TRI reagent (Sigma-Aldrich, Darmstadt, Germany) was used for isolation of RNA from HAECs. RNA was directly converted to cDNA using a cDNA reverse transcription kit (ThermoFisher Scientific, Waltham, MA, USA). TaqMan® Gene Expression Master Mix (ThermoFisher Scientific, Waltham, MA, USA) and pre-designed TaqMan® primers were used for amplification reaction 20ng of cDNA. The relative expression ratio was calculated as described previously (20). GAPDH was used as a reference for normalizing the data.

3.11. Immunofluorescence flow cytometry

After reaching 80-90% confluence, cells (wild type, transfected or not with scrambled RNA (scRNA), KLF6 or endoglin siRNA) were exposed to 7K (5 or 10 µg/mL) for 12 hours with or without 2-hydroxypropyl-β-cyclodextrin (11 hours before experiment) or PHA-408 (12 hours 10 minutes before experiment). Protein expression was evaluated by immunofluorescence flow cytometry analysis.

Direct flow cytometry was used for the detection of ICAM-1 and P/E-selectins on the cell surface. Cells were rinsed with PBS (prepared from tablets; Sigma, Darmstadt, Getmany) after 12 hours of premedication, detached with trypsin (Biosera, Nuaille, France) and incubated with

primary fluorescent-labelled mouse monoclonal antibody against human ICAM-1 (R&D Systems, Minneapolis, MN, USA) or P/E-selectins (R&D Systems, Minneapolis, MN, USA).

Indirect flow cytometry was used for the detection of membrane endoglin. Cells were rinsed with PBS after 12 hours of premedication, detached with trypsin and incubated with primary mouse monoclonal antibody against human endoglin (P4A4; DSHBS, Developmental Studies Hybridoma Bank, The University of Iowa, Iowa, USA). After 1 hour incubation, cells were rinsed with PBS and incubated with secondary goat anti-mouse fluorescent-labelled antibody (Alexa 488, Life Technologies, Foster City, CA, USA).

Intracellular flow cytometry was used for detection of pSmad2/3. Cells were rinsed with PBS and detached with trypsin. Subsequently, cells were fixed with 2% paraformaldehyde and permeabilized with 90% methanol before experiment. After fixation and permeabilization period, the primary rabbit anti-human polyclonal antibody (Cell signaling, Leiden, Netherlands) and fluorescent-labelled secondary chicken anti-rabbit antibody (Invitrogen, Minneapolis, MN, USA) were used.

Determination of protein expression was performed on Cell Lab Quanta SC Flow Cytometer (Beckman Coulter, Inc., California, USA). Results are presented as relative expression index, calculated as percentage of positive cells multiplied by the mean fluorescence intensity (30).

3.12. Cell transfections

HAECs were cultured on six well plates (KLF6 silencing; TPP Sigma-Aldrich, Darmstadt, Getmany) or Petri dishes (endoglin silencing; 60cm^2, VWR) using EGM-2 medium with supplements until 80% confluence. Cells were rinsed with PBS and transfected in serum and antibiotic-free medium with siKLF6 (Santa Cruz, SC-38021, Dallas, TX, USA), siENG (ThermoFisher Scientific, s4679 and s4677, Minneapolis, MN, USA) or scrambled RNA (Sigma-Aldrich, SIC001-1, Darmstadt, Germany) mixed in Opti-MEM™ (ThermoFisher Scientific, Minneapolis, MN, USA) with Lipofectamin 3000 (siKLF6, ThermoFisher Scientific, Minneapolis, MN, USA) or RNAiMAX (siENG, ThermoFisher Scientific, Minneapolis, MN, USA). The final siRNA concentration used for transfections was 16.34 nM/mL. After 5 hours of incubation in medium containing transfection reagents, it was replaced with complete EGM-2

medium containing 10% FBS. Thirty-six hours after transfection, cells were used for experiments according to the manufacturer's guidelines.

3.13. Immunofluorescence microscopy in chamber slides

HAECs were cultured on chamber slides (Eppendorf/SPL, Říčany u Prahy, Czech Republic/Gyeonggi-do, Korea). After reaching 80-90% confluence, cells were treated with 10 μg/mL 7K, alone or in combination with 10μM PHA-408, for 4 hours. Cells were fixed and permeabilized with ice-cold acetone for 10 minutes. After blockage with 5% BSA/0.1% glycine in PBS, cells were incubated with primary rabbit anti-human antibody against RELA (NF-κB p65, Santa Cruz, Dallas, TX, USA) overnight at 4°C. The next morning, cells were rinsed with PBS (Sigma-Aldrich, Darmstadt, Germany) and incubated with secondary chicken anti-rabbit antibody (Invitrogen, Minneapolis, MN, USA).

eNOS, p-eNOS and HO-1 expression was quantified after 2.5 (p-eNOS), 6 (HO-1) or 12 (eNOS) hours treatment with 5 or 10 μg/mL of 7K. After fixation, permeabilization and blocking, cells were incubated with primary rabbit anti-human antibody against eNOS or p-eNOS (both from Santa Cruz, Dallas, TX, USA) or with primary mouse anti-human antibody against HO-1 (Abcam, Cambridge, UK) overnight at 4°C. The next morning, cells were rinsed with PBS (Sigma-Aldrich, Darmstadt, Germany) and incubated with secondary chicken anti-rabbit antibody (Invitrogen, Minneapolis, MN, USA) (eNOS, p-eNOS) or secondary goat anti-mouse antibody (Invitrogen, Minneapolis, MN, USA) (HO-1). After rinsing with PBS, cells were incubated with DAPI (Invitrogen, Minneapolis, MN, USA) for nuclear staining for 5 minutes. Chamber slides were mounted using a solution of 1,4-diazabicyclo[2.2.2]octane (DABCO; Sigma-Aldrich, Dramstadt, Germany) prepared with poly(vinyl alcohol) (Sigma-Aldrich, Darmstadt, Getmany), Tris-HCl (Serva, Heidelberg, Germany) and distilled water. Photomicrographs were obtained using confocal laser scanning microscope system (Nikon A1+, Nikon, Japan) and NIS Elements AR 4.02 software (Laboratory Imaging, Prague, Czech Republic). Six focal planes were imaged to cover the whole volume of the specimen in the field of view using 20× objective lens and 405 and 488 nm lasers together with DAPI and FITC emission filters, respectively. Pinhole was set at 14 μm and laser power was kept as low as possible to prevent any photodamage to the specimen.

3.14. Cell adhesion assays

HAECs were cultured in EGM-2 medium on Petri dishes until 80-90% confluency and exposed, or not, to 10 µg/mL 7K for 12 hours. THP-1 cells were added to HAECs and after 1-hour coincubation, dishes were rinsed using PBS and non-adherent cells were removed. HAECs with adherent THP-1 cells were dissociated using acutase (ThermoFisher Scientific, Minneapolis, MN, USA). The cell mixture was stained on membrane endoglin as mentioned above and analyzed using a flow cytometer and Kaluza software. The method of negative cell sorting was used for detection and counting of the cells. For adhesion experiments on transfected cells, positive sorting of THP-1 monocytes labeled with Vybrant-Dio (3µL/mL 30 minutes before addition to HAECs) in combination with the inhibitor of exocytosis GW4869 (15µM 1 hour before addition to HAECs) was used.

3.15. Cell transmigration assays

Monolayers of HAECs created from normal or transfected cells on the membrane of a transwell insert were used to mimic the endothelium of aorta. HAECs were cultured on membranes of polycarbonate cell culture inserts in multidishes with 3-micron pore size (Nunc^{TM}) until 100% confluency. Then, complete EGM-2 medium (control, siENG group) or EGM-2 with 10µg/mL 7K (7K, siENG+7K group) was added into the lower compartment. Approximately 100,000 of actively proliferating THP-1 cells were added into the upper compartment and after 12 hours of incubation, transmigrated cells were counted in 100µL of medium from the lower compartment using a flow cytometer (Beckman Coulter, Inc., CA, USA) and Kaluza analysis software.

3.16. Statistical analysis

The statistical analysis was performed by GraphPad Prism 7.0 software (GraphPad Software Inc., CA, USA) and GraphPad Outlier calculator. All data are presented as mean ± SEM. All multiple comparisons were analyzed using ANOVA with Kruskal-Wallis test and Dunnett´s multiple comparisons test. Direct group-group comparisons were carried out using Mann-Whitney test. $P \leq 0.05$ was the minimum requirement for a statistically significant difference.

4. RESULTS

4.1. ApoE$^{-/-}$/LDLR$^{-/-}$ mice have elevated cholesterol levels, sEng levels and inflammatory biomarkers in plasma

Biochemical and immunological analyses of cholesterol, sEng and inflammatory biomarkers were performed. We found significantly increased total cholesterol levels (1.53 ± 0.10 vs. 19.0 ± 1.57 mM) between WT and ApoE$^{-/-}$/LDLR$^{-/-}$ mice (Fig. 1A). In parallel with increased total cholesterol concentration, plasma levels of sEng were significantly higher in ApoE$^{-/-}$/LDLR$^{-/-}$ (4,817 ± 341 pg/mL) compared to WT mice (3,010 ± 309 pg/mL) (Fig. 1B). Luminex analysis also showed elevated plasma concentration of P-selectin in the blood of ApoE$^{-/-}$/LDLR$^{-/-}$ (60,013 ± 1,747 pg/mL) compared to WT mice (38,548 ± 3 321 pg/mL) (Fig. 1C).

We examined plasma and urinary levels of (NO_3^-) as a marker of NO metabolism. Determination of NO_3^- plasma concentration showed significant differences between ApoE$^{-/-}$/LDLR$^{-/-}$ and WT mice (34.3 ± 3.10 vs. 65.3 ± 5.25 μM), respectively (Fig. 1D). Urinary NO_3^- excretion was also significantly decreased in ApoE$^{-/-}$/LDLR$^{-/-}$ (524 ± 80.0 μM) compared to WT mice (2,288 ± 206 μM) (Fig. 1E). As expected, ApoE$^{-/-}$/LDLR$^{-/-}$ mice demonstrated a significant decrease in urine creatinine-normalized concentration of NO_3^- compared to WT mice (1.63 ± 0.30 vs. 3.74 ± 0.27 μM/μmol), respectively (Fig. 1F).

4.2. Impaired vascular and endothelial function *ex vivo* in ApoE$^{-/-}$/LDLR$^{-/-}$ mice

Vascular reactivity is primarily evaluated by administration of potassium chloride (KCl) that is able to evoke receptor-independent contraction based on membrane depolarization with subsequent increased cytosolic concentration of Ca^{2+} ions (31). We used KCl in concentration 60 mM to assess the maximal contractile response. As shown in Fig. 2A, the maximal contraction achieved in response to KCl was not significantly different between ApoE$^{-/-}$/LDLR$^{-/-}$ and WT mice (3.56 ± 0.21 vs. 3.78 ± 0.35 mN). Next, increasing concentrations of phenylephrine (PE, 0.01-10 μM), an alpha-adrenergic vasoconstrictor, was used for pre-contraction of aortic rings prior to the next measurements. The maximal induced contraction after administration of PE (10 μM) showed no significant differences between ApoE$^{-/-}$/LDLR$^{-/-}$ and WT mice (35.1 ± 5.70% vs. 27.4 ± 4.48%) (Fig. 2B).

Endothelium-dependent relaxation induced by cumulative concentrations of acetylcholine (Ach, 0.001-0.1 μM) was measured in PE pre-contracted aortic rings. Ach mediates relaxation via activation of muscarinic receptors type III that are responsible for synthesis of NO. We found that the maximal induced relaxation was not significantly different between ApoE$^{-/-}$/LDLR$^{-/-}$ and WT mice (98.7 ± 13.6% vs. 97.1 ± 11.0% at 0.1 μM Ach) (Fig. 2C). For endothelium-independent relaxation, the vasodilator response in PE pre-contracted aortic rings was induced by cumulative concentrations of sodium nitroprusside (SNP, 0.001-0.1 μM), a direct NO donor. The maximal relaxation induced by SNP was significantly impaired in ApoE$^{-/-}$/LDLR$^{-/-}$ compared to WT mice (31.1 ± 9.02 vs. 72.8 ± 8.43% at 0.1 μM SNP) (Fig. 2D). To determine the contribution of other sources of NO, different from the NO generated from L-arginine/eNOS cascade, N (ω)-nitro-L-arginine methyl ester (L-NAME, 300 μM) as a direct inhibitor of eNOS was used (23, 28). The effect of L-NAME on the maximal Ach-induced relaxation in PE pre-contracted aortic rings reached significantly increased values in ApoE$^{-/-}$/LDLR$^{-/-}$ (10.5 ± 4.82%) compared to WT mice (2.44 ± 0.86%) (Fig. 2E).

4.3. Endoglin/Smad2/3/eNOS signaling is impaired in aortas of ApoE$^{-/-}$/LDLR$^{-/-}$ mice

Because Eng regulates protein expression and function of eNOS (9, 10) and is involved in eNOS expression via Smad2/3 transcription factors (32), we examined the protein levels of membrane Eng, eNOS and its active phosphorylated form p-eNOS Ser1177, as well as phosphorylated Smad2/3 (pSmad2/3) in mice aortas. Significantly reduced expression of membrane Eng (to 12%; Fig. 3A), eNOS (to 59%; Fig. 3B), p-eNOS Ser1177 (to 38%; Fig. 3C) and pSmad2/3 (to 71%; Fig. 3D) were observed in aortas of ApoE$^{-/-}$/LDLR$^{-/-}$ mice when compared to WT mice. Next, we determined the protein level of MMP-14 previously reported to be involved in sEng shedding in preeclampsia (33). Interestingly, ApoE$^{-/-}$/LDLR$^{-/-}$ mice displayed a significantly reduced expression of MMP-14 (to 20%; Fig. 3F) compared to WT mice.

Expression of heme oxygenase-1 (HO-1), a carbon monoxide-releasing molecule, was measured to evaluate a possible involvement of this protein in the vasodilatory mechanism leading to an interaction with soluble guanylate cyclase and subsequently to higher NO release

(34). In line with this, we observed a significantly lower expression of HO-1 (to 42%; Fig. 3F) in aortas of $ApoE^{-/-}/LDLR^{-/-}$ mice compared to WT mice.

Myosin light chain (MLC) is a major regulatory component in vascular smooth muscle reactivity. To determine the activation status of MLC, expression of phosphorylated MLC on residues threonine 18 and serine 19 (pMLC Thr18/Ser19) was assessed. As shown in Fig. 3G, significantly lower expression of pMLC Thr18/Ser19 (to 67%) was demonstrated in aortas of $ApoE^{-/-}/LDLR^{-/-}$ mice compared to WT mice.

4.4. 7-ketocholesterol increases endoglin expression and induces endothelial dysfunction in HAECs

To assess whether the oxidized cholesterol contributes to the decrease in endoglin expression of hypercholesterolemic mice, HAECs were incubated with 5 or 10μg/mL of 7-ketocholesterol. Significant increase in both endoglin mRNA (131 ± 8.73% and 138 ± 5.77% of control, respectively, Fig. 4A) and protein (14,123 ± 1,424 and 16,127 ± 1,240, respectively, compared to control 6,853 ± 465) levels was found after 12 hour incubation (Fig. 4B). In addition, a significant dose-dependent increase in endoglin protein levels was demonstrated by immunofluorescence flow cytometry as illustrated by means of representative histograms (Fig. 4C). It is of interest to mention that increase in membrane endoglin protein levels after treatment with 7K was not followed by an increase in sEng levels (243 ± 37.7 pg/mL and 279 ± 54.0 pg/mL, respectively, compared to control 334 ± 11.4 pg/mL) (Fig. 4D). Nevertheless, pSmad2/3 was significantly increased after 7K premedication (95.8 ± 18 and 77.5 ± 16.5 respectively compared to control 29 ± 2.8) (Fig. 4E).

Endothelial dysfunction in vascular endothelium is characterized by increased expression of pro-inflammatory cell adhesion molecules, including ICAM-1 and P/E-selectins. Therefore, we analyzed whether oxysterol treatment affects the expression of these pro-inflammatory markers. Treatment with 7K for 12 hours significantly increased ICAM-1 mRNA expression (148 ± 5.70% and 262 ± 20.5% at 5 and 10μg/mL of 7K, respectively, Fig. 4F). To confirm the hypothesis that 7K treatment can induce an endothelial dysfunction-like phenotype in HAECs, flow cytometry analysis of ICAM-1 and P/E-selectins protein levels was carried out. Protein levels of ICAM-1 were significantly increased at two different doses (5 and 10 μg/mL) of 7K (438 ± 23.3 and 715 ± 98.6, respectively, compared to control 78.7 ± 11.3, Fig. 4G,H). Similarly,

protein levels of P/E-selectins were increased after treatment with 10 μg/mL 7K (97.7 ± 9.2 vs. 45.2 ± 4.22), but not at 5 μg/mL of 7K (Fig. 4I,J). Expression of HO-1 was significantly decreased after 7K treatment (1,923 ± 22.8 and 1,810 ± 18.1, respectively), compared to control values (2,957 ± 29.6) (Fig. 4K).

Activation of eNOS signaling was detected at the mRNA level of eNOS (121.7 ± 4.9% and 176.8 ± 7.3% of control, respectively; Fig. 4L), and protein levels of eNOS (2,412 ± 38 and 2,195 ± 38.6, respectively compared to control 1,120 ± 38; Fig. 4M) and p-eNOS (2,548 ± 11.4 and 2,565 ± 20, respectively compared to control 2,075 ± 14.4; Fig. 4N). Representative confocal microscopy photomicrographs are displayed in Fig. 4O.

4.5. 7-ketocholesterol induces the expression of transcription factors involved in endoglin regulation

It has been demonstrated that endoglin expression is regulated by the activity of different transcription factors, including KLF6 (4, 35), RELA (p65 NF-κB)-HIF-1 (6, 7) and LXR (NR1H3) (8, 36). In agreement with these findings, we found that the expression of the genes encoding these proteins was significantly increased after premedication with 10 μg/mL 7K (127 ± 6.40% for KLF6; 143 ± 4.64% for RELA; and 133 ± 6.44% for NR1H3) (Fig. 5A, B, C).

4.6. KLF6 silencing, cyclodextrins or RELA (NF-κB) inhibition prevent 7-ketocholesterol-induced upregulation of endoglin expression.

Because of the increased expression of KLF6 after 12 hour premedication with 7K in HAECs (Fig. 5A), we investigated further the role of KLF6 in 7K-induced endoglin expression. For this purpose, we used HAECs where the 7K-induced KLF6 mRNA increase was inhibited upon transfection with KLF6 specific siRNA (98.9 ± 2.99% vs 128 ± 6.43%, Fig. 6A). Parallel transfection experiments showed that siKLF6 mRNA was able to prevent 7K-mediated increase in both endoglin mRNA (115 ± 2.96% vs 139 ± 5.80%, Fig. 6B) and endoglin protein (107 ± 24.8% vs 235 ± 18.1%) levels (Fig. 6C,D).

In order to elucidate the role of LXR (NR1H3) in 7K-induced endoglin expression, we used 2-hydroxypropyl-β-cyclodextrin which was able to significantly abolish the 7K-induced gene expression of NR1H3 (LXR) (71.3 ± 2.07% vs 129 ± 6.22%, Fig. 6E). In the same set of experiments, we found that 2-hydroxypropyl-β-cyclodextrin significantly decreased endoglin

gene expression (116 ± 6.10% vs 138 ± 5.78%, Fig. 6F) and endoglin protein levels (87.0 ± 4.80% vs 235 ± 18.1%, Fig. 6G,H) compared to the group premedicated with 7K alone. Our results suggest that this cyclodextrin prevents 7K-induced increase in endoglin expression.

RELA (NF-κB p65) is important for canonical pathway of inflammation (37) and production of hypoxia inducible factor-1α (6, 7), which, in turn, regulates endoglin expression (6). We interfered with RELA (NF-κB) expression by using the IκB kinase-2 inhibitor PHA-408 which decreases translocation of NF-κB to nucleus (38). We found that PHA-408 decreases 7K-induced mRNA expression of RELA (NF-κB) (88.9 ± 3.65% vs 145 ± 4.68%, Fig. 6I), as well as the 7K-induced increase in endoglin mRNA expression (109 ± 6.12% vs 138 ± 5.79%, Fig. 6J) and protein levels (121 ± 9.02% vs 235 ± 18.1%) (Fig. 6K,L).

4.7. Endoglin is involved in 7-ketocholesterol-induced adhesion and transmigration of THP-1 monocytes through HAECs monolayers

THP-1 cell line was used to study the effect of 7K combined with endoglin silencing on the cell permeability across the monolayer formed by HAECs in transwell inserts. Flow cytometry analysis was used to determine the number of adherent and transmigrated THP-1 cells through the endothelial monolayer, whereas inhibition of endoglin expression in HAECs served to elucidate its role in adhesion and transmigration. Endoglin silencing with siRNA resulted in significant reduction of both mRNA (6.63 ± 0.14% and 6.12 ± 0.37% in the presence of 7K, compared to control, Fig. 7A) and protein (177 ± 7.76 and 168 ± 9.29 in the presence of 7K, compared to control 1,705 ± 117 Fig. 7B,C) levels of endoglin and this reduction was not affected upon treatment with 7K. Adhesion studies showed that incubation with 7K increased the number of adherent THP-1 cells on endothelial monolayers (136 ± 6.79% compared to control group), whereas silencing of endoglin in HAECs led to a decreased number of adherent cells, both in the absence (47.9 ± 2.23%) or in the presence of 7K (53.4 ± 0.31%) (Fig. 7D). Similarly, incubation with 7K showed a markedly increased transmigration of THP-1 cells across HAECs (242 ± 15.0%), while endoglin silencing significantly reduced the number of transmigrated cells both in the absence (27.4 ± 2.78%) or in the presence of 7K (40.9 ± 4.14%), suggesting an important role for membrane endothelial endoglin in monocyte transmigration (Fig. 7E).

5. DISCUSSION

Changes of endoglin expression in endothelium reflect potential pathological conditions in the cardiovascular system. Our previous papers suggest that hypercholesterolemia and progression of atherosclerosis are related to the reduced expression of endoglin in mice aorta (19, 39). Moreover it was demonstrated that membrane endoglin/Smad2/3 signaling affects eNOS expression and stability (32) and reduced endoglin expression results in impaired eNOS-dependent vasodilatation (9, 10). Recently, we showed that a combination of high soluble endoglin levels and mild hypercholesterolemia results in aggravation of the vascular function in aorta, with alterations of the endoglin/Smad2/3/eNOS signaling (28). Taken together, we might propose that alteration in endoglin expression is related to potential development/progression of endothelial dysfunction suggesting that endoglin acts as a protective agent in endothelium.

At variance with the vasoprotective role of endoglin, Rossi et al. showed a regulatory role for endoglin in transendothelial leukocyte trafficking (11). These pro-inflammatory effects of endoglin suggest that endoglin could also have a proatherogenic role. However, it is of interest to mention that the *in vivo* experiments in the above-mentioned study were focused on endoglin effects in the microcirculation. In addition, these experiments were performed in a short time-frame (hours), which points out to acute experimental conditions. This is a completely different experimental setting when compared to those studies where the long-term effect of endoglin is analyzed in the macrocirculation, e.g. aorta and/or renal artery. In this study, we set two different biological experiments to assess changes of endoglin expression, regulation and signaling with respect to endothelial/vascular dysfunction, both *in vivo* and *in vitro* under the cholesterol/hypercholesterolemia condition.

Nowadays, little is known about the possible relationship between endoglin expression/signaling and endothelial/vascular dysfunction *in vivo* under hypercholesterolemia. Thus, we used young (2 months old) $ApoE^{-/-}/LDLR^{-/-}$ mice (23) without detectable atherogenic changes in aorta in order to evaluate membrane endoglin/Smad2/3/eNOS signaling with respect to the functional condition of aorta. Our results showed that spontaneous hypercholesterolemia in $ApoE^{-/-}/LDLR^{-/-}$ mice is accompanied by increased levels of the pro-inflammatory biomarker P-selectin, reduced urine and plasma concentration of NO_3^- and increased levels of sEng, suggesting the early development of endothelial dysfunction in these mice without detectable atherosclerosis.

High levels of sEng might be considered as a biomarker of early endothelial/vascular dysfunction/alteration and vascular damage in many cardiovascular disorders in clinical conditions. It was shown that sEng is generated by the cleavage from membrane-bound endoglin by MMP-14 which was proposed to be the major endoglin shedding protease (3). Surprisingly, we found significantly reduced expression of MMP-14 in aortas of $ApoE^{-/-}/LDLR^{-/-}$ mice, suggesting that MMP-14 is unlikely to be responsible for the cleavage of membrane endoglin in aorta in these mice. Indeed, similar results were also shown by Brownfoot et al., suggesting that other matrix metalloproteinases could be involved in the cleavage of membrane endoglin (40). Moreover, it is unlikely that changes of sEng levels reflect changes of membrane endoglin expression in only one vessel type, e.g. aorta. Instead, we propose that sEng is released from the whole vasculature in cardiovascular diseases. Indeed, we have demonstrated that hypercholesteremia reduces membrane (aortic) endoglin, but increases the levels of circulating endoglin (19). In addition, membrane endoglin/Smad2/3/eNOS signaling was related to vascular reactivity and NO-dependent vasodilation (9, 10). We showed that membrane endoglin/Smad2/3/eNOS is altered and related to aggravation of endothelial dysfunction in mice exposed to high levels of sEng and mild hypercholesterolemia (28). Indeed, expression of membrane endoglin, pSmad2/3, eNOS and p-eNOS Ser1177 was reduced in hypercholesterolemic $ApoE^{-/-}/LDLR^{-/-}$ mice when compared to normocholesterolemic mice in this paper. Noteworthy, reduced NO_3^- levels, as a stable end-product of NO metabolism, is a hallmark of endothelial dysfunction(41, 42). In line with this, we observed a reduced expression of HO-1 in $ApoE^{-/-}/LDLR^{-/-}$ mice aorta, which is involved in a vasodilatory mechanism based on an interaction with soluble guanylate cyclase and a subsequent release of NO (34). Taken together, these data suggest a lower production of NO in $ApoE^{-/-}/LDLR^{-/-}$ mice when compared to control normocholesterolemic mice when endoglin signaling is compromised.

In order to elucidate functional consequences of these changes, we evaluated vascular reactivity of aortic rings by wire myograph. The results showed no changes in acetylcholine-induced relaxation, but demonstrated reduced relaxation induced by SNP and increased relaxation response in $ApoE^{-/-}/LDLR^{-/-}$ mice after L-NAME, suggesting an altered vascular function in these hypercholesterolemic mice. The response to L-NAME probably reflects an ongoing compensatory mechanism (generating NO) to maintain the physiological relaxation in the aortas of $ApoE^{-/-}/LDLR^{-/-}$ mice. We also observed a reduced expression of pMLC

Thr18/Ser19 that is considered a major regulatory component in smooth muscle reactivity (43). Taken together, hypercholesterolemic mice have altered endoglin expression and signaling in aorta, reduced NO levels accompanied by alteration of vascular function in aorta. Thus, we postulate that the reduced endoglin levels are related to vascular dysfunction in aorta prior formation of atherosclerotic lesion, suggesting an important role for endoglin in cholesterol-induced endothelial/vascular dysfunction.

In the second part of the study, we aimed to elucidate endoglin regulation/expression in endothelial cells *in vitro* when simulating hypercholesterolemia by 7K treatment. We were curious to know whether endoglin is similarly regulated as *in vivo* in "atherogenesis/endothelial dysfunction" experiments.

Increased concentrations of oxLDL represent a major risk factor for the development of atherosclerosis (44, 45). Among the different oxysterols present in oxLDL, 7K has been shown to be more abundant in the circulation of patients with hypercholesterolemia (14) and in atherosclerotic lesions than any other oxysterol species (46). In addition, 7K potentiates inflammation (16) and foam cell formation (17), decreases eNOS activity and impairs nitric oxide bioavailability in endothelium (47). Therefore, 7K was used to mimic hypercholesterolemic and proatherogenic condition of oxLDL in our *in vitro* experimental settings. Our results showed that 7K increased the expression of endoglin (opposite to hypercholesterolemia in *in vivo* experiments), as well as biomarkers of endothelial dysfunction and inflammation ICAM-1 and P/E selectins in HAECs. These findings are in agreement with the active role of oxysterols in inflammatory diseases (48) and with the upregulated expression of endoglin upon treatment with 22(R)-hydroxycholesterol and LXR agonists (36, 49). In addition, we demonstrated that the endoglin/pSmad2/3/eNOS/p-eNOS signaling cascade is activated in HAECs by 7K. These above results on endoglin signaling suggest a completely opposite effect of cholesterol exposure *in vivo* and *in vitro*.

Moreover, 7K was able to increase the expression of transcription factors regulating endoglin expression in our study, including KLF6 (4, 35), LXR (NR1H3) (49) and RELA (NFkB) (6, 7). Since 7-ketocholesterol was able to upregulate these three pathways responsible for regulating endoglin expression, we aimed to evaluate whether they were also involved in the regulation of endoglin expression under 7K exposure.

KLF6 is well known for its role in regulating endoglin expression (4, 35) and we have shown that silencing of KLF6 prevents 7K-mediated increase in both endoglin mRNA and protein levels. Interestingly, co-transfection of RAW264.7 cells with KLF6 and NF-κB p65 showed an enhanced inflammatory reaction of cells after LPS treatment, suggesting an interplay between KLF6 and NF-κB p65 in inflammatory settings (50, 51). Of note, RELA (NF-κB p65) is key for the canonical pathway of inflammation (37) and production of HIF-1α (6, 7). In turn, HIF-1α, in combination with Sp1 and Smad3, is able to induce endoglin expression (6), suggesting, that an activation of RELA mRNA expression is indirectly responsible for the 7K-mediated increase in endoglin mRNA expression and endoglin protein levels observed in this study. Supporting this view, we interfered with RELA expression using the IκB kinase-2 inhibitor PHA-408 (38), leading to a decreased translocation of NF-κB to the nucleus, and preventing the 7K-induced increase in endoglin mRNA expression and endoglin protein levels, as well.

The oxysterol receptor LXR is able to bind LXR response elements in the endoglin promoter and mediate the activation of endoglin gene expression (36). To affect LXR mRNA expression, we used 2-hydroxypropyl-β-cyclodextrin. Cyclodextrins are known to extract cholesterol from cells (52) and increase activity of LXR in a time-dependent fashion; thus, they are able to increase LXR mRNA expression a few minutes or hours after administration (53). In our study, treatment with 2-hydroxypropyl-β-cyclodextrin for 11 hours decreased LXR activity (52) and prevented 7K-induced increase in endoglin expression. It is of interest to mention that cyclodextrin also disrupts caveolae on the cell surface of endothelial cells and it is well known that endoglin is present in caveolae (9), so the inhibitory effect on endoglin expression could also be due to depletion of endoglin-containing caveolae. Taken together, our results show that endoglin expression in HAECs is regulated by three transcription factors: KLF6, NF-κB and LXR and that inhibition of each of these factors results in prevention of 7K-induced endoglin expression.

What are the functional consequences of changes in endoglin expression with respect to potential atherogenesis? Transmigration of monocytes is one of the first steps in the development of endothelial dysfunction. Monocytes show hypercholesterolemia-associated trafficking through the endothelial monolayer, subendothelial accumulation and differentiation, which results in formation of foam cells (54-56) and later on they participate in the progression of

atherosclerosis. Therefore, we tried to evaluate a possible link between 7K-induced endoglin expression and the adhesion/transmigration of monocytes across the HAECs monolayer. We showed that 7K-induced expression of endoglin was accompanied by increased adhesion and transmigration of monocytes, whilst inhibition of endoglin expression prevented the 7K-induced adhesion and transmigration. These data suggest that endoglin plays a relevant role in oxysterol-induced trafficking of monocytes through the endothelial monolayer *in vitro*. This interpretation agrees with the reported role for endoglin in integrin-mediated leukocyte adhesion and extravasation induced by inflammation (11).

Our current study shows differences in endoglin expression after cholesterol exposure *in vivo* in aorta and *in vitro* in aortic endothelial cells. Several explanations may account for these apparent discrepancies. First, endoglin is a part of TGF-β signaling pathway and it has been demonstrated that the role of TGF-β varies during atherogenesis. Thus, TGF-β is proatherogenic in the early phase (57), but anti-atherogenic at later stages (58). In other words, endoglin expression may vary during the different stages of atherogenic process/endothelial dysfunction as well. Second, *in vitro* experiments analyze changes of endoglin expression and its consequences within hours, whilst *in vivo* experiments are carried out in two-month-old animals. This discrepancy deserves further investigation, especially focusing on timeline changes of endoglin expression and functional consequences during the atherogenic process. Third, the animal model used in this study is deficient in LDL receptors and therefore, the uptake of cholesterols/oxysterols might be inhibited, and so is the LXR intracellular pathway that triggers endoglin expression. This point deserves further investigation as well. Moreover, not all the oxysterol types behave the same and it is difficult to compare this *in vitro* result with the *in vivo* result with hypercholesterolemic mice. *In vivo*, a variety of oxysterol species are present, and they may act in concert or even in synergy, leading to a different outcome than the one induced by a single oxysterol species. Finally, the other significant difference between our *in vitro* and *in vivo* experiments is that LDL cholesterol in mice contains not only cholesterol, but also apolipoprotein B 100 (ApoB-100)-containing particles. Interestingly, several studies indicated that ApoB-100 seems to be at least a co-factor in endothelial dysfunction development besides cholesterol (59, 60), suggesting that the presence of complex lipoproteins in *in vivo* experiments might be responsible as well for different findings when compared to *in vitro* results . Thus, we will also focus on apoB effects on HAECs in our prospective experiments.

There are possible limitations in this study. First, we cannot confirm our *in vivo* results about endoglin role in the development of endothelial/vascular dysfunction by using endoglin knockout mice because these mice die in utero (61) and, to the best of our knowledge, no hypercholesterolemic endoglin knock out animal model is available. The second potential limitation is related to our *in vitro* experiments. It is not feasible to use general oxLDL (that would mimic hypercholesterolemic conditions from our mice experiments) in our *in vitro* experiments. Particles of oxLDL include different amounts of phospholipids, sphingolipids, free fatty acids, oxysterols, cholesteryl esters, apolipoproteins and other biologically active compounds affecting vascular cell wall. However it is not possible to carry out *in vitro* experiments with these oxLDL particles due to their instability, autooxidation, aggregation, and fusion, among others (14). Thus, 7-ketocholesterol, the most abundant oxysterol of oxLDL (62), was used in our *in vitro* experiments.

6. CONCLUSION

We showed for the first time that hypercholesterolemia altered endoglin expression and signaling, followed by endothelial/vascular dysfunction before the formation of atherosclerotic lesions in $ApoE^{-/-}/LDLR^{-/-}$ mice. By contrast, 7-ketocholesterol increased endoglin expression, and induced inflammation in cultured HAECs, which was followed by an increase in adhesion and transmigration of monocytes via endothelium, that was prevented by endoglin inhibition. Thus, we propose a relevant role for endoglin in endothelial/vascular dysfunction/inflammation when exposed to cholesterol. Nevertheless, due to discrepancies between *in vivo* and *in vitro* results, we propose to be cautious when interpreting data about the role of endoglin in endothelial/vascular dysfunction/inflammation from "acute" *in vitro* experiments or microcirculation studies when compared to long term experiments in large atherosclerosis prone blood vessels.

ACKNOWLEDGMENTS

We thank Mgr. Alena Mrkvicová Ph.D. and Milena Hajzlerová for assistance during PCR analysis, RnDr. Veronika Skarková Ph.D. for assistance during Elisa analysis and preparation of samples for western blots, Mgr. Soňa Čejková Ph.D. and Feroz Ahmad Ph.D. for help with THP-1 cell line, Mgr. Petra Hiršová Ph.D. for information about immunocytochemistry, Pharmdr.

Hana Jansová Ph.D. for help with preparation of substances for cell treatments, RnDr. Věra Králová Ph.D. for help with flow cytometry and Pavlína Lukešová for help during chamber slide preparation.

SOURCES OF FUNDING

This work was supported by project EFSA-CDN (No. CZ.02.1.01/0.0/0.0/16_019/0000841) co-funded by ERDF, grants of Charles University Grant Agency, GAUK 1158413C, 1216217, Specific University Research SVV/2017/260414 and Czech Health Research Council (AZV CR 17-31754A). CB was supported by grants from *Consejo Superior de Investigaciones Cientificas* (201420E039) and *Centro de Investigacion Biomedica en Red de Enfermedades Raras* (CIBERER; ISCIII-CB06/07/0038). CIBERER is an initiative of the *Instituto de Salud Carlos III* (ISCIII) of Spain supported by FEDER funds.

AUTHOR CONTRIBUTIONS

M. Vicen, B. Vitverova, P. Nachtigal designed research and analyzed data; M. Vicen, B. Vitverova, R. Havelek, K. Blazickova, M. Machacek, performed research; all authors wrote the paper.

DISCLOSURES

None.

REFERENCES

1. Nachtigal, P., Zemankova Vecerova, L., Rathouska, J., and Strasky, Z. (2012) The role of endoglin in atherosclerosis. *Atherosclerosis* **224**, 4-11
2. Venkatesha, S., Toporsian, M., Lam, C., Hanai, J., Mammoto, T., Kim, Y. M., Bdolah, Y., Lim, K. H., Yuan, H. T., Libermann, T. A., Stillman, I. E., Roberts, D., D'Amore, P. A., Epstein, F. H., Sellke, F. W., Romero, R., Sukhatme, V. P., Letarte, M., and Karumanchi, S. A. (2006) Soluble endoglin contributes to the pathogenesis of preeclampsia. *Nat Med* **12**, 642-649
3. Hawinkels, L. J., Kuiper, P., Wiercinska, E., Verspaget, H. W., Liu, Z., Pardali, E., Sier, C. F., and ten Dijke, P. (2010) Matrix metalloproteinase-14 (MT1-MMP)-mediated endoglin shedding inhibits tumor angiogenesis. *Cancer Res* **70**, 4141-4150
4. Botella, L. M., Sanchez-Elsner, T., Sanz-Rodriguez, F., Kojima, S., Shimada, J., Guerrero-Esteo, M., Cooreman, M. P., Ratziu, V., Langa, C., Vary, C. P., Ramirez, J. R., Friedman, S., and Bernabeu, C. (2002) Transcriptional activation of endoglin and transforming growth factor-beta signaling components by cooperative interaction between Sp1 and KLF6: their potential role in the response to vascular injury. *Blood* **100**, 4001-4010
5. Ollauri-Ibanez, C., Lopez-Novoa, J. M., and Pericacho, M. (2017) Endoglin-based biological therapy in the treatment of angiogenesis-dependent pathologies. *Expert Opin Biol Ther* **17**, 1053-1063
6. Sanchez-Elsner, T., Botella, L. M., Velasco, B., Langa, C., and Bernabeu, C. (2002) Endoglin expression is regulated by transcriptional cooperation between the hypoxia and transforming growth factor-beta pathways. *J Biol Chem* **277**, 43799-43808
7. van Uden, P., Kenneth, N. S., and Rocha, S. (2008) Regulation of hypoxia-inducible factor-1alpha by NF-kappaB. *Biochem J* **412**, 477-484
8. Valbuena-Diez, A. C., Blanco, F.J., Oujo, B. et al. (2012) Oxysterol-induced soluble endoglin release and its involment in hypertension. In *Circulation* pp. 2612-2624
9. Toporsian, M., Gros, R., Kabir, M. G., Vera, S., Govindaraju, K., Eidelman, D. H., Husain, M., and Letarte, M. (2005) A role for endoglin in coupling eNOS activity and

regulating vascular tone revealed in hereditary hemorrhagic telangiectasia. *Circ Res* **96**, 684-692

10. Jerkic, M., Rivas-Elena, J. V., Prieto, M., Carron, R., Sanz-Rodriguez, F., Perez-Barriocanal, F., Rodriguez-Barbero, A., Bernabeu, C., and Lopez-Novoa, J. M. (2004) Endoglin regulates nitric oxide-dependent vasodilatation. *FASEB J* **18**, 609-611
11. Rossi, E., Sanz-Rodriguez, F., Eleno, N., Duwell, A., Blanco, F. J., Langa, C., Botella, L. M., Cabanas, C., Lopez-Novoa, J. M., and Bernabeu, C. (2013) Endothelial endoglin is involved in inflammation: role in leukocyte adhesion and transmigration. *Blood* **121**, 403-415
12. Rossi, E., Pericacho, M., Bachelot-Loza, C., Pidard, D., Gaussem, P., Poirault-Chassac, S., Blanco, F. J., Langa, C., Gonzalez-Manchon, C., Novoa, J. M. L., Smadja, D. M., and Bernabeu, C. (2018) Human endoglin as a potential new partner involved in platelet-endothelium interactions. *Cell Mol Life Sci* **75**, 1269-1284
13. Steinberg, D. (2002) Atherogenesis in perspective: hypercholesterolemia and inflammation as partners in crime. *Nat Med* **8**, 1211-1217
14. Levitan, I., Volkov, S., Subbaiah, P.V. (2010) Oxidized LDL: Diversity, Patterns of Recognition, and Pathophysiology. In *Antioxidants & Redox Signaling* pp. 39-75
15. Chalubinski, M., Zemanek, K., Skowron, W., Wojdan, K., Gorzelak, P., and Broncel, M. (2013) The effect of 7-ketocholesterol and 25-hydroxycholesterol on the integrity of the human aortic endothelial and intestinal epithelial barriers. *Inflamm Res* **62**, 1015-1023
16. Olkkonen, V. M., Beaslas, O., Nissila, E. (2012) Oxysterols and their cellular effectors. In *Biomolecules* pp. 76-103
17. Hayden, J. M., Brachova, L., Higgins, K., Obermiller, L., Sevanian, A., Khandrika, S., and Reaven, P. D. (2002) Induction of monocyte differentiation and foam cell formation in vitro by 7-ketocholesterol. *J Lipid Res* **43**, 26-35
18. Rathouska, J., Jezkova, K., Nemeckova, I., and Nachtigal, P. (2015) Soluble endoglin, hypercholesterolemia and endothelial dysfunction. *Atherosclerosis* **243**, 383-388
19. Strasky, Z., Vecerova, L., Rathouska, J., Slanarova, M., Brcakova, E., Kudlackova, Z., Andrys, C., Micuda, S., and Nachtigal, P. (2011) Cholesterol effects on endoglin and its downstream pathways in ApoE/LDLR double knockout mice. *Circ J* **75**, 1747-1755

20. Zemankova, L., Varejckova, M., Dolezalova, E., Fikrova, P., Jezkova, K., Rathouska, J., Cerveny, L., Botella, L. M., Bernabeu, C., Nemeckova, I., and Nachtigal, P. (2015) Atorvastatin-induced endothelial nitric oxide synthase expression in endothelial cells is mediated by endoglin. *J Physiol Pharmacol* **66**, 403-413
21. Ruiz-Remolina, L., Ollauri-Ibanez, C., Perez-Roque, L., Nunez-Gomez, E., Perez-Barriocanal, F., Lopez-Novoa, J. M., Pericacho, M., and Rodriguez-Barbero, A. (2017) Circulating soluble endoglin modifies the inflammatory response in mice. *PLoS One* **12**, e0188204
22. Ishibashi, S., Herz, J., Maeda, N., Goldstein, J. L., and Brown, M. S. (1994) The two-receptor model of lipoprotein clearance: tests of the hypothesis in "knockout" mice lacking the low density lipoprotein receptor, apolipoprotein E, or both proteins. *Proc Natl Acad Sci U S A* **91**, 4431-4435
23. Csanyi, G., Gajda, M., Franczyk-Zarow, M., Kostogrys, R., Gwozdz, P., Mateuszuk, L., Sternak, M., Wojcik, L., Zalewska, T., Walski, M., and Chlopicki, S. (2012) Functional alterations in endothelial NO, PGI(2) and EDHF pathways in aorta in ApoE/LDLR-/- mice. *Prostaglandins & other lipid mediators* **98**, 107-115
24. Jawien, J., Csanyi, G., Gajda, M., Mateuszuk, L., Lomnicka, M., Korbut, R., and Chlopicki, S. (2007) Ticlopidine attenuates progression of atherosclerosis in apolipoprotein E and low density lipoprotein receptor double knockout mice. *Eur J Pharmacol* **556**, 129-135
25. Yamagata, K., Tanaka, N., and Suzuki, K. (2013) Epigallocatechin 3-gallate inhibits 7-ketocholesterol-induced monocyte-endothelial cell adhesion. *Microvasc Res* **88**, 25-31
26. Kij, A., Mateuszuk, L., Sitek, B., Przyborowski, K., Zakrzewska, A., Wandzel, K., Walczak, M., and Chlopicki, S. (2016) Simultaneous quantification of PGI2 and TXA2 metabolites in plasma and urine in NO-deficient mice by a novel UHPLC/MS/MS method. *J Pharm Biomed Anal* **129**, 148-154
27. Przyborowski, K., Wojewoda, M., Sitek, B., Zakrzewska, A., Kij, A., Wandzel, K., Zoladz, J. A., and Chlopicki, S. (2015) Effects of 1-Methylnicotinamide (MNA) on Exercise Capacity and Endothelial Response in Diabetic Mice. *PLoS One* **10**, e0130908
28. Vitverova, B., Blazickova, K., Najmanova, I., Vicen, M., Hyspler, R., Dolezelova, E., Nemeckova, I., Tebbens, J. D., Bernabeu, C., Pericacho, M., and Nachtigal, P. (2018)

Soluble endoglin and hypercholesterolemia aggravate endothelial and vessel wall dysfunction in mouse aorta. *Atherosclerosis* **271**, 15-25

29. Nemeckova, I., Serwadczak, A., Oujo, B., Jezkova, K., Rathouska, J., Fikrova, P., Varejckova, M., Bernabeu, C., Lopez-Novoa, J. M., Chlopicki, S., and Nachtigal, P. (2015) High soluble endoglin levels do not induce endothelial dysfunction in mouse aorta. *PLoS One* **10**, e0119665
30. Puig-Kroger, A., Relloso, M., Fernandez-Capetillo, O., Zubiaga, A., Silva, A., Bernabeu, C., and Corbi, A. L. (2001) Extracellular signal-regulated protein kinase signaling pathway negatively regulates the phenotypic and functional maturation of monocyte-derived human dendritic cells. *Blood* **98**, 2175-2182
31. Dopico, A. M., Bukiya, A. N., and Jaggar, J. H. (2018) Calcium- and voltage-gated BK channels in vascular smooth muscle. *Pflugers Arch*
32. Santibanez, J. F., Letamendia, A., Perez-Barriocanal, F., Silvestri, C., Saura, M., Vary, C. P., Lopez-Novoa, J. M., Attisano, L., and Bernabeu, C. (2007) Endoglin increases eNOS expression by modulating Smad2 protein levels and Smad2-dependent TGF-beta signaling. *J Cell Physiol* **210**, 456-468
33. Kaitu'u-Lino, T. J., Palmer, K. R., Whitehead, C. L., Williams, E., Lappas, M., and Tong, S. (2012) MMP-14 Is Expressed in Preeclamptic Placentas and Mediates Release of Soluble Endoglin. *American Journal of Pathology* **180**, 888-894
34. Kaczara, P., Proniewski, B., Lovejoy, C., Kus, K., Motterlini, R., Abramov, A. Y., and Chlopicki, S. (2018) CORM-401 induces calcium signalling, NO increase and activation of pentose phosphate pathway in endothelial cells. *FEBS J* **285**, 1346-1358
35. Gallardo-Vara, E., Blanco, F. J., Roque, M., Friedman, S. L., Suzuki, T., Botella, L. M., and Bernabeu, C. (2016) Transcription factor KLF6 upregulates expression of metalloprotease MMP14 and subsequent release of soluble endoglin during vascular injury. *Angiogenesis* **19**, 155-171
36. Henry-Berger, J., Mouzat, K., Baron, S., Bernabeu, C., Marceau, G., Saru, J. P., Sapin, V., Lobaccaro, J. M., and Caira, F. (2008) Endoglin (CD105) expression is regulated by the liver X receptor alpha (NR1H3) in human trophoblast cell line JAR. *Biol Reprod* **78**, 968-975

37. Lawrence, T. (2009) The nuclear factor NF-kappaB pathway in inflammation. *Cold Spring Harb Perspect Biol* **1**, a001651
38. Mbalaviele, G., Sommers, C. D., Bonar, S. L., Mathialagan, S., Schindler, J. F., Guzova, J. A., Shaffer, A. F., Melton, M. A., Christine, L. J., Tripp, C. S., Chiang, P. C., Thompson, D. C., Hu, Y., and Kishore, N. (2009) A novel, highly selective, tight binding IkappaB kinase-2 (IKK-2) inhibitor: a tool to correlate IKK-2 activity to the fate and functions of the components of the nuclear factor-kappaB pathway in arthritis-relevant cells and animal models. *J Pharmacol Exp Ther* **329**, 14-25
39. Vecerova, L., Strasky, Z., Rathouska, J., Slanarova, M., Brcakova, E., Micuda, S., and Nachtigal, P. (2012) Activation of TGF-beta receptors and Smad proteins by atorvastatin is related to reduced atherogenesis in ApoE/LDLR double knockout mice. *J Atheroscler Thromb* **19**, 115-126
40. Brownfoot, F. C., Hannan, N., Onda, K., Tong, S., and Kaitu'u-Lino, T. (2014) Soluble endoglin production is upregulated by oxysterols but not quenched by pravastatin in primary placental and endothelial cells. *Placenta* **35**, 724-731
41. Heitzer, T., Schlinzig, T., Krohn, K., Meinertz, T., and Munzel, T. (2001) Endothelial dysfunction, oxidative stress, and risk of cardiovascular events in patients with coronary artery disease. *Circulation* **104**, 2673-2678
42. Kleinbongard, P., Dejam, A., Lauer, T., Jax, T., Kerber, S., Gharini, P., Balzer, J., Zotz, R. B., Scharf, R. E., Willers, R., Schechter, A. N., Feelisch, M., and Kelm, M. (2006) Plasma nitrite concentrations reflect the degree of endothelial dysfunction in humans. *Free Radical Bio Med* **40**, 295-302
43. Somlyo, A. P., and Somlyo, A. V. (1994) Signal transduction and regulation in smooth muscle. *Nature* **372**, 231-236
44. Friedman, A., and Hao, W. (2015) A mathematical model of atherosclerosis with reverse cholesterol transport and associated risk factors. *Bull Math Biol* **77**, 758-781
45. Mitra, S., Goyal, T., and Mehta, J. L. (2011) Oxidized LDL, LOX-1 and atherosclerosis. *Cardiovasc Drugs Ther* **25**, 419-429
46. Vaya, J., Aviram, M., Mahmood, S., Hayek, T., Grenadir, E., Hoffman, A., and Milo, S. (2001) Selective distribution of oxysterols in atherosclerotic lesions and human plasma lipoproteins. *Free Radic Res* **34**, 485-497

47. Deckert, V., Persegol, L., Viens, L., Lizard, G., Athias, A., Lallemant, C., Gambert, P., and Lagrost, L. (1997) Inhibitors of arterial relaxation among components of human oxidized low-density lipoproteins. Cholesterol derivatives oxidized in position 7 are potent inhibitors of endothelium-dependent relaxation. *Circulation* **95**, 723-731
48. Testa, G., Rossin, D., Poli, G., Biasi, F., and Leonarduzzi, G. (2018) Implication of oxysterols in chronic inflammatory human diseases. *Biochimie* **153**, 220-231
49. Valbuena-Diez, A. C., Blanco, F. J., Oujo, B., Langa, C., Gonzalez-Nunez, M., Llano, E., Pendas, A. M., Diaz, M., Castrillo, A., Lopez-Novoa, J. M., and Bernabeu, C. (2012) Oxysterol-induced soluble endoglin release and its involvement in hypertension. *Circulation* **126**, 2612-2624
50. Date, D., Das, R., Narla, G., Simon, D. I., Jain, M. K., and Mahabeleshwar, G. H. (2014) Kruppel-like transcription factor 6 regulates inflammatory macrophage polarization. *J Biol Chem* **289**, 10318-10329
51. Zhang, Y., Lei, C. Q., Hu, Y. H., Xia, T., Li, M., Zhong, B., and Shu, H. B. (2014) Kruppel-like factor 6 is a co-activator of NF-kappaB that mediates p65-dependent transcription of selected downstream genes. *J Biol Chem* **289**, 12876-12885
52. Coisne, C., Hallier-Vanuxeem, D., Boucau, M. C., Hachani, J., Tilloy, S., Bricout, H., Monflier, E., Wils, D., Serpelloni, M., Parissaux, X., Fenart, L., and Gosselet, F. (2016) beta-Cyclodextrins Decrease Cholesterol Release and ABC-Associated Transporter Expression in Smooth Muscle Cells and Aortic Endothelial Cells. *Front Physiol* **7**, 185
53. Coisne, C., Tilloy, S., Monflier, E., Wils, D., Fenart, L., and Gosselet, F. (2016) Cyclodextrins as Emerging Therapeutic Tools in the Treatment of Cholesterol-Associated Vascular and Neurodegenerative Diseases. *Molecules* **21**
54. Carman, C. V. (2008) Teasing out monocyte trafficking mechanisms. *Blood* **112**, 929-930
55. Mestas, J., and Ley, K. (2008) Monocyte-endothelial cell interactions in the development of atherosclerosis. *Trends Cardiovasc Med* **18**, 228-232
56. Woollard, K. J., and Geissmann, F. (2010) Monocytes in atherosclerosis: subsets and functions. *Nat Rev Cardiol* **7**, 77-86
57. Majesky, M. W., Lindner, V., Twardzik, D. R., Schwartz, S. M., and Reidy, M. A. (1991) Production of transforming growth factor beta 1 during repair of arterial injury. *J Clin Invest* **88**, 904-910

58. Gojova, A., Brun, V., Esposito, B., Cottrez, F., Gourdy, P., Ardouin, P., Tedgui, A., Mallat, Z., and Groux, H. (2003) Specific abrogation of transforming growth factor-beta signaling in T cells alters atherosclerotic lesion size and composition in mice. *Blood* **102**, 4052-4058
59. Yu, Q., Zhang, Y., and Xu, C. B. (2015) Apolipoprotein B, the villain in the drama? *Eur J Pharmacol* **748**, 166-169
60. Zhang, Y., Zhang, W., Edvinsson, L., and Xu, C. B. (2014) Apolipoprotein B of low-density lipoprotein impairs nitric oxide-mediated endothelium-dependent relaxation in rat mesenteric arteries. *Eur J Pharmacol* **725**, 10-17
61. van Laake, L. W., van den Driesche, S., Post, S., Feijen, A., Jansen, M. A., Driessens, M. H., Mager, J. J., Snijder, R. J., Westermann, C. J., Doevendans, P. A., van Echteld, C. J., ten Dijke, P., Arthur, H. M., Goumans, M. J., Lebrin, F., and Mummery, C. L. (2006) Endoglin has a crucial role in blood cell-mediated vascular repair. *Circulation* **114**, 2288-2297
62. Brown, A. J., Mander, E. L., Gelissen, I. C., Kritharides, L., Dean, R. T., and Jessup, W. (2000) Cholesterol and oxysterol metabolism and subcellular distribution in macrophage foam cells. Accumulation of oxidized esters in lysosomes. *J Lipid Res* **41**, 226-237

Fig. 1: Biochemical and Luminex analyses of plasma. Plasma concentration of total cholesterol (A), mouse sEng (B), P-selectin (C), NO3- in plasma (D), NO3- in urine (E) and urine creatinine-normalized concentration of NO3- (F) in ApoE-/-/LDLR-/- and WT mice. Data are shown as mean ± S.E.M., Mann-Whitney test, *p ≤ 0.05, **p ≤ 0.01, ***p ≤ 0.001. n = 7 mice per group.

Fig. 2: Vasomotor function evaluation of aorta. Maximal contraction to KCl (60 mM) (A), PE-induced contraction (B), Ach-induced relaxation in PE pre-contracted aortic rings (C), SNP-induced relaxation in PE pre-contracted aortic rings (D) and inhibitory effect of L-NAME on eNOS-dependent Ach-induced relaxation in PE pre-contracted aortic rings (E) in ApoE-/-/LDLR-/- and WT mice. Data are shown as mean ± S.E.M., Mann-Whitney test, *p ≤ 0.05. n = 7 mice per group.

Fig. 3: Western blot analysis of aortas from ApoE-/-/LDLR-/- and WT mice. The expression of membrane Eng (A), eNOS (B), p-eNOS-Ser1177 (C), pSmad2/3 (D), MMP-14 (E), HO-1 (F) and pMLC Thr18/Ser19 (G) in total protein extracts from mice aortas. Top: densitometric analysis (control = 100%). Equal loading of samples was confirmed by immunodetection of GAPDH. Bottom: representative immunoblots. Data are shown as mean ± S.E.M., Mann-Whitney test, *p ≤ 0.05, **p ≤ 0.01. n = 7 mice per group.

Fig. 4: Effect of oxysterol on the expression of endoglin, pSmad2/3, ICAM-1, P/E-selectins, HO-1, eNOS and p-eNOS in HAECs. Untreated HAECs (Control) and premedicated HAECs for 12 hours with 5 or 10 µg/mL 7K were analyzed for mRNA and protein expression, as indicated. Endoglin mRNA expression (A). Endoglin protein levels (B,C). sENG protein levels (D). pSmad2/3 protein levels (E), ICAM-1 mRNA expression (F), protein levels (G,H). P/E-selectins protein levels (I,J). HO-1 protein levels (K), eNOS mRNA expression (L) and protein levels (M). p-eNOS protein levels (N). HO-1, eNOS and p-eNOS protein levels were calculated from confocal microscopy photomicrographs (O) as described in Materials and methods. DAPI (blue) - nuclei; Alexa Fluor 488 (green) - HO-1/eNOS/p-eNOS respectively. Bar represents 100 µm. Data are shown as mean ± S.E.M., ANOVA with Kruskal-Wallis test followed Dunn's multiple

comparisons test, *p ≤ 0.05, **p ≤ 0.01, ***p ≤ 0.001. n = 5-208 measurements from 3 independent cell stocks.

Fig. 5: Effect of 7-ketocholesterol on mRNA levels of transcription factors that regulate endoglin expression. mRNA expression of KLF6 (A), NR1H3 (LXR) (B) and RELA (NF-κB) (C) in control group and groups premedicated for 12 hours with 5 or 10 μg/mL 7K, as indicated. Data are shown as mean ± S.E.M., ANOVA with Kruskal-Wallis test followed Dunn's multiple comparisons test, *p ≤ 0.05, **p ≤ 0.01, ***p ≤ 0.001. n = 18-24 measurements from 3 independent cell stocks.

Fig. 6: Effect of KLF6 silencing, cyclodextrins or RELA (NF-κB) inhibition on 7-ketocholesterol-induced endoglin expression in HAECs. Cells were untreated (Control) or premedicated with 10 μg/mL 7K for 12 hours, as indicated. A-D. HAECs were transfected with siKLF6 mRNA prior treatment with 7K, and expression of KLF6 mRNA (A), endoglin mRNA (B) and endoglin protein (C,D) was determined. E-H. HAECs were incubated with 10 mM 2-hydroxypropyl-β-cyclodextrin for 11 hours prior treatment with 7K, and expression of NR1H3(LXR) mRNA (E), endoglin mRNA (F) and endoglin protein (G,H) was determined. I-N. HAECs were premedicated with 10 μM PHA-408 for 10 minutes before addition of 7K, and expression of RELA (NF-κB) mRNA (I), endoglin mRNA (J) and endoglin protein (K,L). RELA (NF-κB) protein levels (M) were calculated from confocal microscopy photomicrographs (N) as described in Materials and methods. DAPI (blue) - nuclei; Alexa Fluor 488 (green) - RELA (NF-κB). Bar represents 100 μm. Data are shown as mean ± S.E.M., ANOVA followed by Bonferroni's multiple comparisons test, *p ≤ 0.05, **p ≤ 0.01, ***p ≤ 0.001. n = 5-224 measurements from 3 independent cell stocks.

Fig. 7: Effect of endoglin silencing on adhesion and transmigration of THP-1 cells through HAECs monolayers. HAECs were transfected with endoglin siRNAs or scRNA (control group) for 48 hours and then premedicated with 10 μg/mL of 7K for 12 hours, as indicated. The expression of endoglin mRNA (A) and endoglin protein levels (B) was measured using flow cytometry (C). The number of adherent cells (D) was quantified using Kaluza software and the number of transmigrated cells (E) was determined in 100 μl of culture media from the lower

compartment of the transwell using flow cytometry. Data are shown as mean ± S.E.M., ANOVA with Kruskal-Wallis test followed Dunn's multiple comparisons test, *$p \leq 0.05$, **$p \leq 0.01$, ***$p \leq 0.001$. n = 6-12 measurements from 3 independent cell stocks.

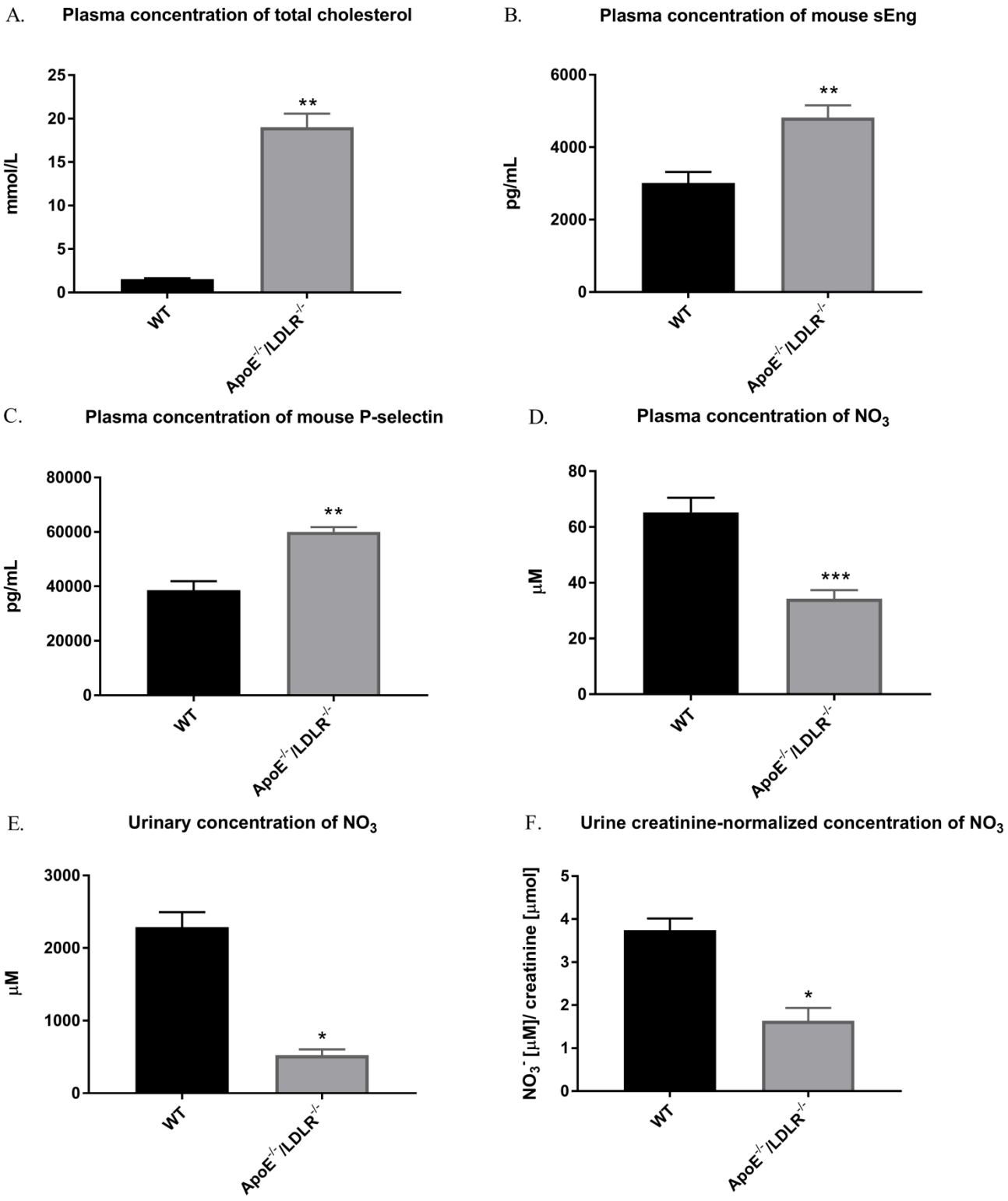
A.
Plasma concentration of total cholesterol
mmol/L
25
20
15
10
5
0
**
WT
ApoE-/-/LDLR-/-
B.
Plasma concentration of mouse sEng
pg/mL
6000
4000
2000
0
**
WT
ApoE-/-/LDLR-/-
C.
Plasma concentration of mouse P-selectin
pg/mL
80000
60000
40000
20000
0
**
WT
ApoE-/-/LDLR-/-
D.
Plasma concentration of NO3
µM
80
60
40
20
0
***
WT
ApoE-/-/LDLR-/-
E.
Urinary concentration of NO3
µM
3000
2000
1000
0
*
WT
ApoE-/-/LDLR-/-
F.
Urine creatinine-normalized concentration of NO3
NO3- [µM]/ creatinine [µmol]
5
4
3
2
1
0
*
WT
ApoE-/-/LDLR-/-

Figure 1

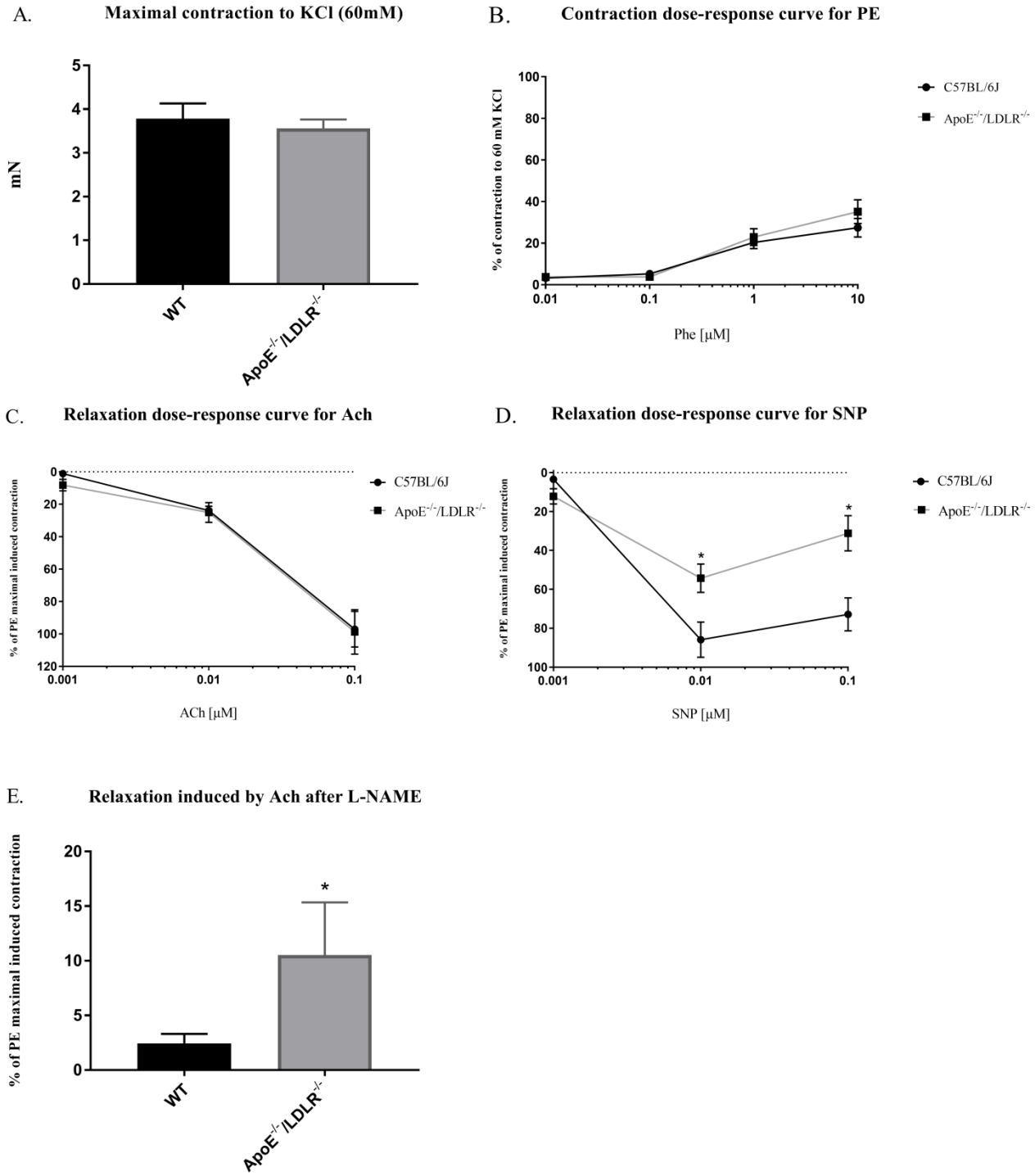
A.
Maximal contraction to KCl (60mM)
mN
5
4
3
2
1
0
WT
ApoE-/-/LDLR-/-
B.
Contraction dose-response curve for PE
% of contraction to 60 mM KCl
100
80
60
40
20
0
0.01
0.1
1
10
Phe [µM]
C57BL/6J
ApoE-/-/LDLR-/-
C.
Relaxation dose-response curve for Ach
% of PE maximal induced contraction
0
20
40
60
80
100
120
0.001
0.01
0.1
ACh [µM]
C57BL/6J
ApoE-/-/LDLR-/-
D.
Relaxation dose-response curve for SNP
% of PE maximal induced contraction
0
20
40
60
80
100
0.001
0.01
0.1
*
*
SNP [µM]
C57BL/6J
ApoE-/-/LDLR-/-
E.
Relaxation induced by Ach after L-NAME
% of PE maximal induced contraction
20
15
10
5
0
*
WT
ApoE-/-/LDLR-/-

Figure 2

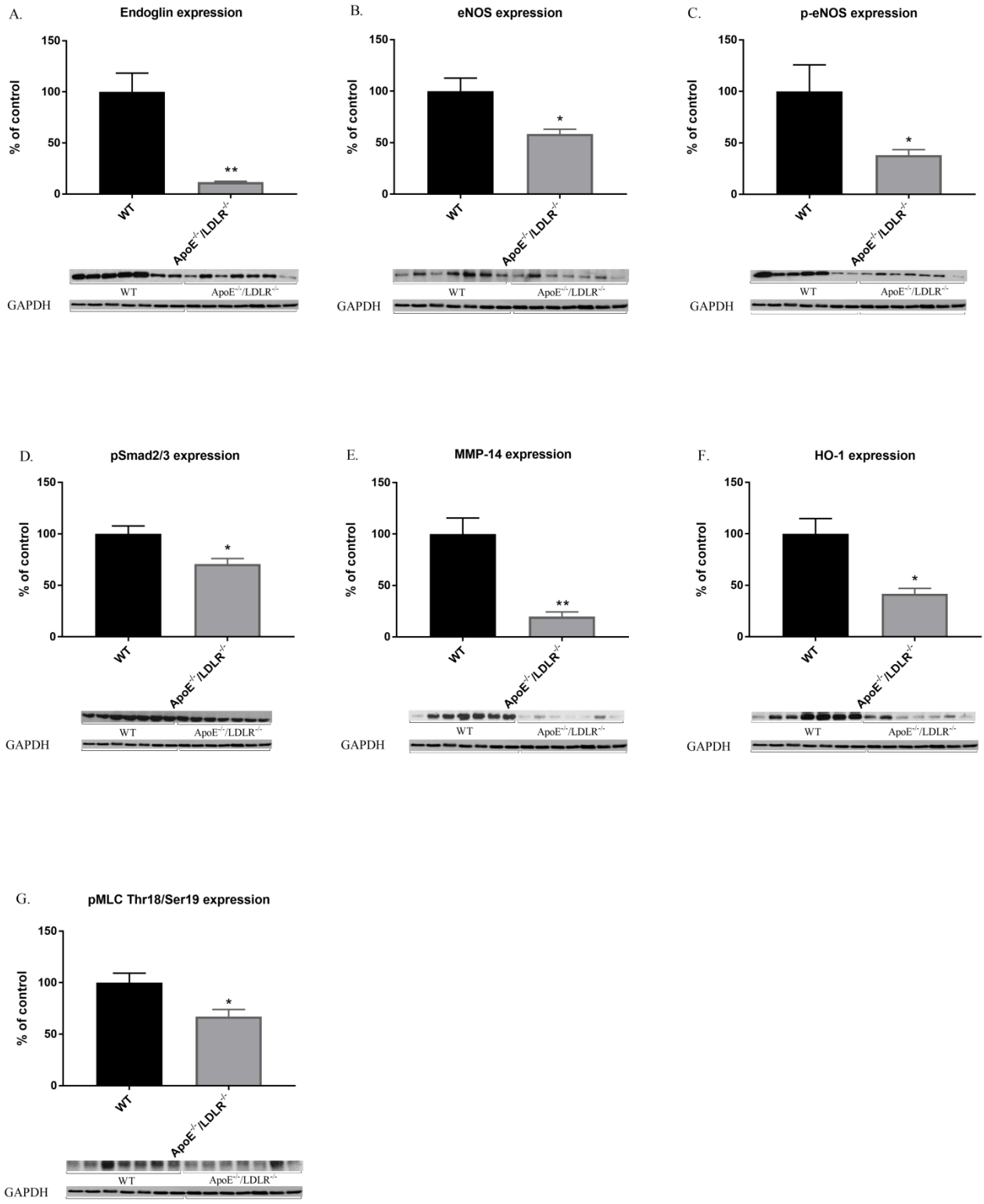
A.
Endoglin expression
% of control
150
100
50
0
**
WT
ApoE-/-/LDLR-/-
WT
ApoE-/-/LDLR-/-
GAPDH
B.
eNOS expression
% of control
150
100
50
0
*
WT
ApoE-/-/LDLR-/-
WT
ApoE-/-/LDLR-/-
GAPDH
C.
p-eNOS expression
% of control
150
100
50
0
*
WT
ApoE-/-/LDLR-/-
WT
ApoE-/-/LDLR-/-
GAPDH
D.
pSmad2/3 expression
% of control
150
100
50
0
*
WT
ApoE-/-/LDLR-/-
WT
ApoE-/-/LDLR-/-
GAPDH
E.
MMP-14 expression
% of control
150
100
50
0
**
WT
ApoE-/-/LDLR-/-
WT
ApoE-/-/LDLR-/-
GAPDH
F.
HO-1 expression
% of control
150
100
50
0
*
WT
ApoE-/-/LDLR-/-
WT
ApoE-/-/LDLR-/-
GAPDH
G.
pMLC Thr18/Ser19 expression
% of control
150
100
50
0
*
WT
ApoE-/-/LDLR-/-
WT
ApoE-/-/LDLR-/-
GAPDH

Figure 3

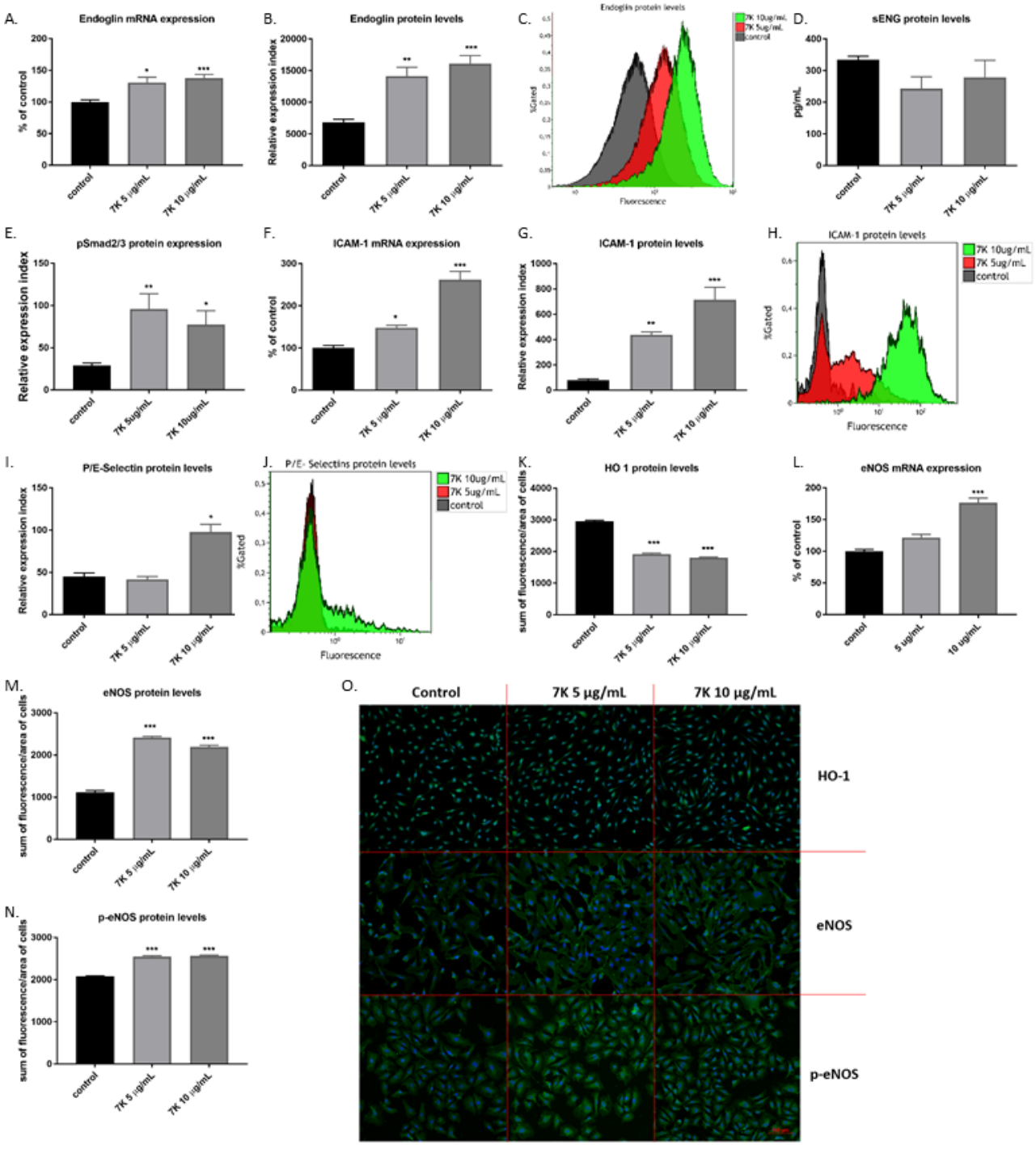
A.
Endoglin mRNA expression
% of control
control
7K 5 µg/mL
7K 10 µg/mL
B.
Endoglin protein levels
Relative expression index
C.
Endoglin protein levels
7K 10ug/mL
7K 5ug/mL
control
%Gated
Fluorescence
D.
sENG protein levels
pg/mL
E.
pSmad2/3 protein expression
Relative expression index
7K 5ug/mL
7K 10ug/mL
F.
ICAM-1 mRNA expression
G.
ICAM-1 protein levels
H.
ICAM-1 protein levels
I.
P/E-Selectin protein levels
J.
P/E- Selectins protein levels
K.
HO 1 protein levels
sum of fluorescence/area of cells
L.
eNOS mRNA expression
5 ug/mL
10 ug/mL
M.
eNOS protein levels
N.
p-eNOS protein levels
O.
Control
7K 5 µg/mL
7K 10 µg/mL
HO-1
eNOS
p-eNOS

Figure 4

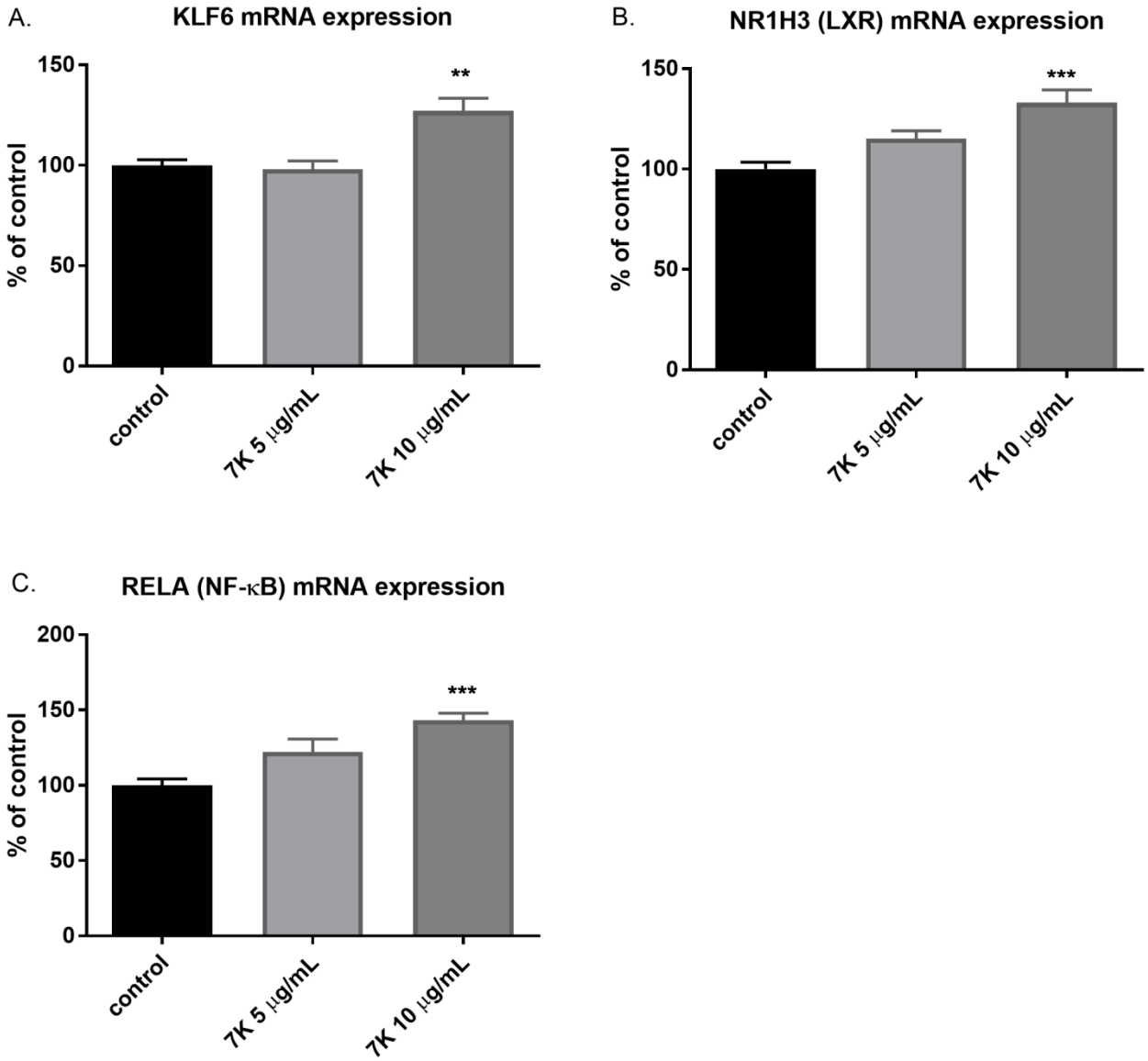
A.
KLF6 mRNA expression
% of control
150
100
50
0
**
control
7K 5 μg/mL
7K 10 μg/mL
B.
NR1H3 (LXR) mRNA expression
% of control
150
100
50
0
***
control
7K 5 μg/mL
7K 10 μg/mL
C.
RELA (NF-κB) mRNA expression
% of control
200
150
100
50
0
***
control
7K 5 μg/mL
7K 10 μg/mL

Figure 5

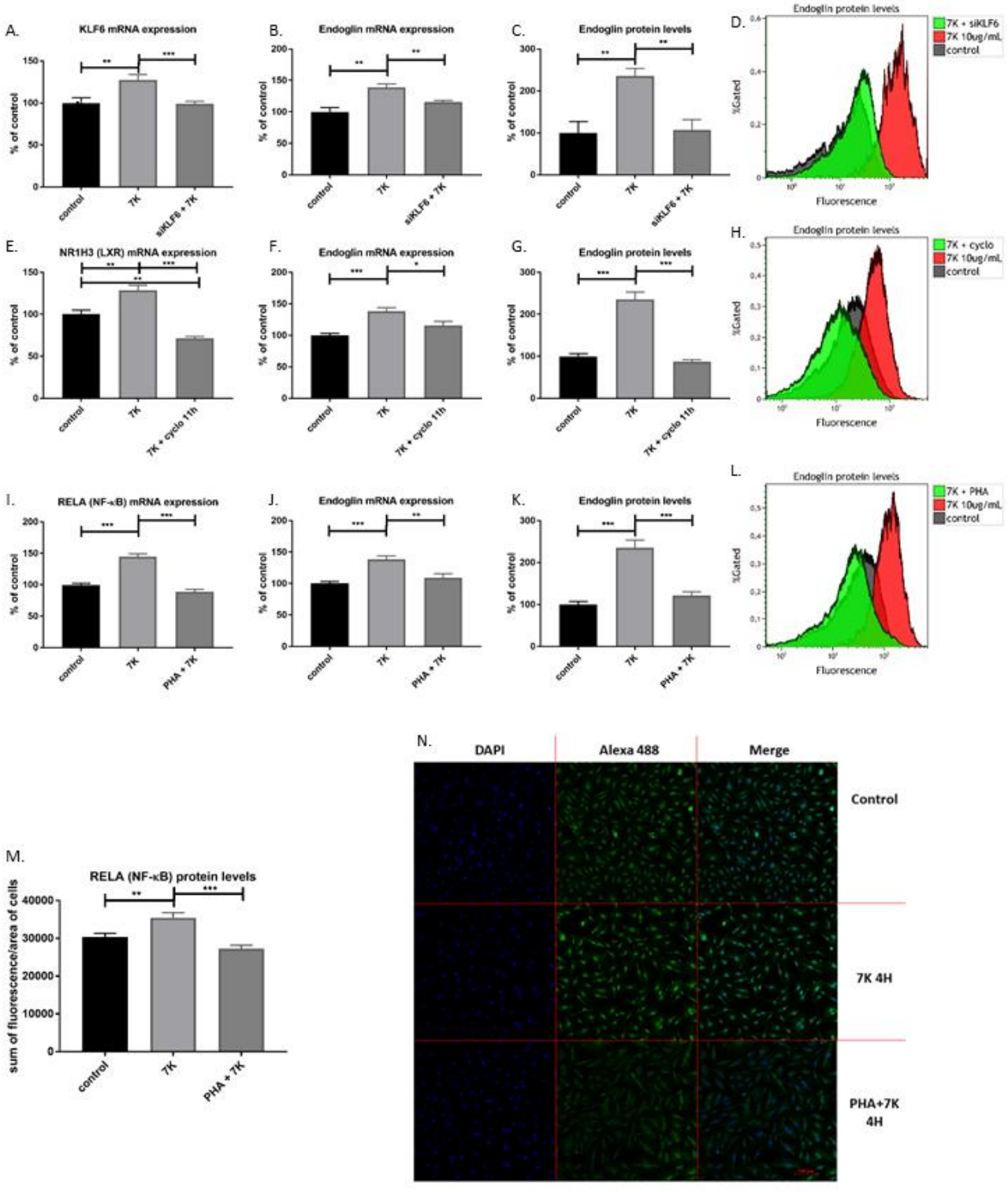
A.
KLF6 mRNA expression
% of control
control
7K
siKLF6 + 7K
B.
Endoglin mRNA expression
C.
Endoglin protein levels
D.
Endoglin protein levels
7K + siKLF6
7K 10ug/mL
control
%Gated
Fluorescence
E.
NR1H3 (LXR) mRNA expression
7K + cyclo 11h
F.
Endoglin mRNA expression
G.
Endoglin protein levels
H.
Endoglin protein levels
7K + cyclo
I.
RELA (NF-κB) mRNA expression
PHA + 7K
J.
Endoglin mRNA expression
K.
Endoglin protein levels
L.
Endoglin protein levels
7K + PHA
M.
RELA (NF-κB) protein levels
sum of fluorescence/area of cells
N.
DAPI
Alexa 488
Merge
Control
7K 4H
PHA+7K 4H

Figure 6

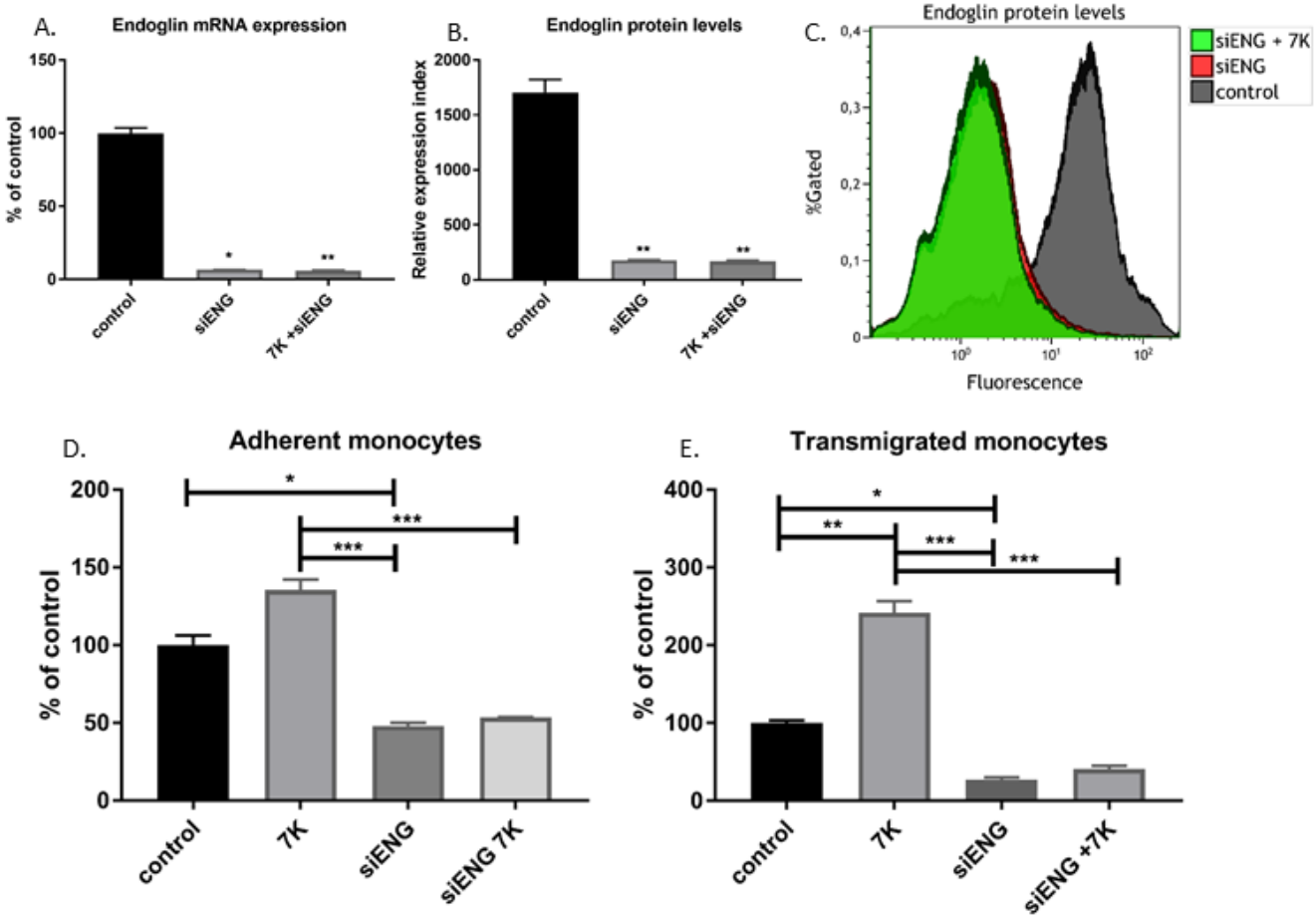
A.
Endoglin mRNA expression
% of control
150
100
50
0
*
**
control
siENG
7K +siENG
B.
Endoglin protein levels
Relative expression index
2000
1500
1000
500
0
**
**
control
siENG
7K +siENG
C.
Endoglin protein levels
%Gated
0,4
0,3
0,2
0,1
0
Fluorescence
siENG + 7K
siENG
control
D.
Adherent monocytes
% of control
200
150
100
50
0
*
***
***
control
7K
siENG
siENG 7K
E.
Transmigrated monocytes
% of control
400
300
200
100
0
*
**
***
***
control
7K
siENG
siENG +7K

Figure 7